Journal of Human Genetics (2011) 56, 707–715

www.nature.com/jhg

ORIGINAL ARTICLE

HRAS mutants identified in Costello syndrome patients can induce cellular senescence: possible implications for the pathogenesis of Costello syndrome

Tetsuya Niihori[1], Yoko Aoki[1], Nobuhiko Okamoto[2], Kenji Kurosawa[3], Hirofumi Ohashi[4], Seiji Mizuno[5], Hiroshi Kawame[6], Johji Inazawa[7], Toshihiro Ohura[8], Hiroshi Arai[9], Shin Nabatame[10], Kiyoshi Kikuchi[11], Yoshikazu Kuroki[12], Masaru Miura[13], Toju Tanaka[14], Akira Ohtake[15], Isaku Omori[16], Kenji Ihara[17], Hiroyo Mabe[18], Kyoko Watanabe[19], Shinichi Niijima[20], Erika Okano[21], Hironao Numabe[22] and Yoichi Matsubara[1]

Costello syndrome (CS) is a congenital disease that is characterized by a distinctive facial appearance, failure to thrive, mental retardation and cardiomyopathy. In 2005, we discovered that heterozygous germline mutations in *HRAS* caused CS. Several studies have shown that CS-associated *HRAS* mutations are clustered in codons 12 and 13, and mutations in other codons have also been identified. However, a comprehensive comparison of the substitutions identified in patients with CS has not been conducted. In the current study, we identified four mutations (p.G12S, p.G12A, p.G12C and p.G12D) in 21 patients and analyzed the associated clinical manifestations of CS in these individuals. To examine functional differences among the identified mutations, we characterized a total of nine HRAS mutants, including seven distinct substitutions in codons 12 and 13, p.K117R and p.A146T. The p.A146T mutant demonstrated the weakest Raf-binding activity, and the p.K117R and p.A146T mutants had weaker effects on downstream c-Jun N-terminal kinase signaling than did codon 12 or 13 mutants. We demonstrated that these mutant HRAS proteins induced senescence when overexpressed in human fibroblasts. Oncogene-induced senescence is a cellular reaction that controls cell proliferation in response to oncogenic mutation and it has been considered one of the tumor suppression mechanisms *in vivo*. Our findings suggest that the *HRAS* mutations identified in CS are sufficient to cause oncogene-induced senescence and that cellular senescence might therefore contribute to the pathogenesis of CS.
Journal of Human Genetics (2011) **56**, 707–715; doi:10.1038/jhg.2011.85; published online 18 August 2011

Keywords: Costello syndrome; HRAS; phenotype-genotype; RAS/MAPK; senescence

INTRODUCTION

Costello syndrome (CS, OMIM 218040) is a genetic disorder that is characterized by a distinctive facial appearance, loose skin, failure to thrive, mental retardation, cardiomyopathy and a predisposition to tumor formation.[1] Patients with CS have an estimated 13% chance of developing tumors, usually rhabdomyosarcoma, neuroblastoma or bladder cancer.[2] Previously, we identified heterozygous germline *HRAS* mutations in patients with CS.[3] It has been suggested that the CS diagnosis should be applied only to patients with a mutation in *HRAS* because of the high risk of malignancies associated with *HRAS* mutations and the relative homogeneity of the CS phenotype.[4]

[1]Department of Medical Genetics, Tohoku University School of Medicine, Sendai, Japan; [2]Department of Medical Genetics, Osaka Medical Center and Research Institute for Maternal and Child Health, Izumi, Japan; [3]Division of Medical Genetics, Kanagawa Children's Medical Center, Yokohama, Japan; [4]Division of Medical Genetics, Saitama Children's Medical Center, Saitama, Japan; [5]Department of Pediatrics, Central Hospital, Aichi Human Service Center, Kasugai, Japan; [6]Department of Genetic Counseling, Ochanomizu University, Tokyo, Japan; [7]Department of Molecular Cytogenetics, Medical Research Institute and School of Biomedical Science, Tokyo Medical and Dental University, Tokyo, Japan; [8]Division of Pediatrics, Sendai City Hospital, Sendai, Japan; [9]Department of Pediatric Neurology, Morinomiya Hospital, Osaka, Japan; [10]Department of Child Neurology, National Center Hospital (NCH), National Center of Neurology and Psychiatry, Tokyo, Japan; [11]Department of Pediatrics, Shimane Prefectural Central Hospital, Izumo, Japan; [12]Department of Neonatology, Kurashiki Central Hospital, Kurashiki, Japan; [13]Division of Cardiology, Tokyo Metropolitan Children's Medical Center, Tokyo, Japan; [14]Division of Clinical Genetics and Molecular Medicine, National Research Institute for Child Health and Development, Tokyo, Japan; [15]Department of Pediatrics, Saitama Medical University, Moroyama, Japan; [16]Department of Neonatology, Center for Maternal, Fetal & Neonatal Medicine, Tokyo Metropolitan Bokutoh Hospital, Tokyo, Japan; [17]Department of Pediatrics, Graduate School of Medical Sciences, Kyushu University, Fukuoka, Japan; [18]Department of Child Development, Faculty of Life Sciences, Kumamoto University, Kumamoto, Japan; [19]Division of Pediatrics, National Hospital Organization Kokura Medical Center, Kitakyushu, Japan; [20]Department of Pediatrics, Juntendo University, Nerima Hospital, Tokyo, Japan; [21]Department of Pediatrics, Jikei University School of Medicine, Tokyo, Japan and [22]Department of Clinical Genetics, Kyoto University Hospital, Kyoto, Japan

Correspondence: Dr T Niihori or Dr Y Aoki, Department of Medical Genetics, Tohoku University School of Medicine, 1-1 Seiryo-machi, Sendai 980-8574, Japan.
E-mail: tniihori@med.tohoku.ac.jp or aokiy@med.tohoku.ac.jp
Received 4 April 2011; revised and accepted 15 June 2011; published online 18 August 2011

A total of 14 *HRAS* missense mutations and one duplication mutation have been reported in 185 patients with CS[3,5–23] or congenital myopathy with excess of muscle spindles.[24] Most of these mutations have previously been reported as somatic and oncogenic mutations in various tumors. More than 90% of the mutations found in CS patients are clustered in codons 12 and 13 (p.G12A/S/V/C/D/E and p.G13C/D). Other mutations, including p.Q22K, p.E37dup, p.T58I, p.E63K, p.K117R, p.A146V and p.A146T, have also been identified, albeit rarely. Although the clinical manifestations of CS appear to be homogeneous, several genotype-phenotype correlations have been reported. Previous studies have also suggested that CS patients with the p.G12A mutation may have an increased risk of malignancy, compared with patients with p.G12S.[7] Patients with the p.G12C mutation had a more severe CS phenotype; these individuals developed severe hypertrophic cardiomyopathy and died in the neonatal period. Patients with p.K117R or p.A146V had a milder and more unusual CS phenotype, compared with patients with mutations in codon 12 or 13. Though detailed analyses of some mutants have been performed,[13,25–28] a comprehensive comparison of the substitutions identified in patients with CS has not been conducted.

The activated RAS/mitogen-activated protein kinase (MAPK) pathway generally stimulates cell proliferation, but it can also result in antiproliferation under certain conditions. Overexpressing HRAS p.G12V in human and murine fibroblasts caused oncogene-induced senescence (OIS),[29–31] which protects cells from proliferating in the presence of oncogene-induced damage.[32,33] OIS is a cellular reaction that controls cell proliferation in response to oncogenic mutation and is considered a tumor suppression mechanism *in vivo*.[34,35] Studies of a zebrafish model of CS, which expresses *HRAS* p.G12V, have shown that progenitor cells in the adult heart and brain undergo cellular senescence, suggesting that OIS in adult progenitor cells contributes to the development of CS. We hypothesized that OIS would be a key mechanism of the clinical manifestations in patients with CS, including short stature, osteoporosis and tumor suppressive effects. However, it has not been verified that HRAS mutants other than p.G12V cause cellular senescence.

The three aims of this study were the following: (1) to examine the detailed clinical manifestations of CS in patients with *HRAS* mutations, (2) to characterize a large panel of HRAS mutants to look for differences among various mutations located in codon 12/13 and to compare the effects of mutants in codon 12/13 with those of p.K117R/p.A146T, and (3) to clarify whether *HRAS* mutants other than p.G12V can cause OIS. To address these issues, we analyzed the *HRAS* mutations in CS patients and studied the Raf-binding activity, downstream signaling and ability to cause senescence of a large panel of HRAS mutants.

MATERIALS AND METHODS

Patients

A total of 31 patients suspected of having CS were recruited to the study. The diagnosis of CS was evaluated by clinical geneticists. All patients had sporadic cases. The study was approved by the Ethics Committee of the Tohoku University School of Medicine.

Mutation analysis

We sequenced the *HRAS* genes of all patients in the study to confirm the diagnosis of CS. After obtaining written informed consent, genomic DNA was isolated from the peripheral leukocytes of patients. Four coding exons of *HRAS* from 31 CS patients were sequenced. Each *HRAS* exon with flanking intronic sequences was amplified using primers based on sequences obtained from GenBank (GenBank accession no. NT035113). The M13 reverse or forward sequence was added to the 5′ end of the polymerase chain reaction primers for use, as a sequencing. polymerase chain reaction was performed in a 30 µl reaction containing 10 mM Tris-HCl (pH 8.3), 50 mM KCl, 1.5 mM $MgCl_2$, 0.2 mM deoxyribonucleotide triphosphate, 10% (v/v) dimethyl sulfoxide, 0.4 pmol each primer, 100 ng genomic DNA and 2.5 units of Taq DNA polymerase. The reaction consisted of 35 cycles of denaturation at 94 °C for 15 s, annealing at 57 °C for 15 s and extension at 72 °C for 30 s. The products were gel-purified and sequenced on an Applied Biosystems 3130 Genetic Analyzer (Applied Biosystems, Foster City, CA, USA).

Plasmids

To introduce exogenous wild-type or mutated HRAS into cultured cells, we constructed plasmids encoding wild-type or mutant *HRAS* cDNAs. Human *HRAS* cDNA in pUSEamp was purchased from Upstate Biotechnology (Lake Placid, NY, USA). The plasmid was digested with *Eco*RI and subcloned into pBluescript KSII+ (Stratagene, La Jolla, CA, USA). Substitutions generating p.G12V (c.35G>T), p.G12A (c.35G>C), p.G12S (c.34G>A), p.G12C (c.34G>C), p.G12D (c.35G>A), p.G13C (c.37G>C), p.G13D (c.38G>A), p.K117R (c.350A>G) or p.A146T (c.436G>A) were introduced using the QuikChange Site-Directed mutagenesis kit (Stratagene). All mutant and wild-type constructs were verified by sequencing. The full-length wild-type and mutant *HRAS* cDNAs were digested with *Eco*RI and subcloned into the pBabe-puro retroviral vector (GenHunter, Nashville, TN, USA) and the pCAGGS expression vector (gifted by Dr Jun-ichi Miyazaki of Osaka University). The pBabe-zeo-Ecotropic Receptor plasmid (Addgene plasmid 10687, Addgene Inc., Cambridge, MA, USA) was obtained from Addgene.

Cell culture and senescence-associated β-galactosidase staining

NIH 3T3 cells, human fibroblast BJ cells and the Phoenix Ampho and Eco packaging cell lines were purchased from the American Tissue Culture Collection (Manassas, VA, USA). NIH 3T3 cells were maintained in Dulbecco's modified Eagle medium containing 10% calf serum, 100 U/ml penicillin and 100 µg/ml streptomycin. BJ and Phoenix cells were maintained in Dulbecco's modified Eagle medium containing 10% fetal calf serum, 100 U/ml penicillin and 100 µg/ml streptomycin. To characterize the phenotypes of cells overexpressing wild-type or mutated HRAS, senescence associated β-galactosidase staining was performed with the Senescence β-Galactosidase Staining Kit (Cell Signaling Technology, Beverly, MA, USA) according to the manufacturer's protocol.

Ras activation assay

We performed RAS activation assays to clarify the functional differences among the HRAS mutants identified in patients with CS. The Ras activation assay kit was purchased from Millipore (Billerica, MA, USA). NIH 3T3 cells were plated in 6-well plates at 1.5×10^5 cells per well. Cells were transfected using Lipofectamine Plus (Invitrogen, Carlsbad, CA, USA) with 1 µg wild-type or mutant *HRAS* construct. The assay was performed according to the manufacturer's protocol.

Luciferase assay

We used luciferase assays to examine the effect of the identified mutations on the RAS pathway. NIH 3T3 cells were plated in 12-well plates at 1×10^5 cells per well. After 24 h, cells were transiently transfected with 700 ng pFR-luc, 10 ng pFA2-Elk1 or 10 ng pFA2-cJun, 7 ng phRLnull-luc and 35 ng wild-type or mutant *HRAS* construct, using Lipofectamine Plus (Invitrogen). At 18 h after transfection, the cells were serum starved in Dulbecco's modified Eagle medium for 24 h. Cells were then harvested in passive lysis buffer, and luciferase activity was assayed using the Promega Dual-Luciferase assay kit (Promega, Madison, WI, USA). Renilla luciferase expressed by phRLnull-luc was used to normalize the transfection efficiency. The experiments were performed in triplicate. Statistical analysis was performed with Tukey's multiple comparison test.

Western blotting

We performed western blotting against molecular markers of premature senescence to confirm their expression in cells overexpressing HRAS. Cells were harvested at the indicated times, washed in ice-cold phosphate-buffered saline and lysed on ice in lysis buffer (10 mM Tris-HCl, pH 7.5 and 1% sodium

dodecyl sulfate). Lysates were boiled for 5 min and centrifuged at 13 000 *g* for 10 min at 4 °C. Protein concentrations were estimated using the Lowry or Bradford method (BioRad, Hercules, CA, USA), and each lysate was adjusted to equalize the protein concentrations. Equal volumes of lysates were mixed with 2×sodium dodecyl sulfate sample buffer and boiled for 5 min. Electrophoresis was performed on 5–15% sodium dodecyl sulfate–polyacrylamide gels. After separation, proteins were transferred to nitrocellulose membranes. The membranes were blocked in 5% non-fat dry milk in Tris-buffered saline with 0.1% Tween 20 for 1 h at room temperature and incubated overnight at 4 °C with one of the following primary antibodies: HRAS (sc-520, Santa Cruz Biotechnology, Santa Cruz, CA, USA), phospho-p44/42MAPK, p44/42MAPK (#9102 and #9101, respectively, Cell Signaling Technology, Danvers, MA, USA), p16 (sc-468, Santa Cruz Biotechnology), phospho-p53 (Ser15) (#9284, Cell Signaling Technology) or β-actin (A5316, Sigma, St. Louis, MO, USA). Detection was performed using the enhanced chemiluminescence method (Amersham, GE Healthcare UK, Amersham, UK), with the appropriate peroxidase-conjugated secondary antibody.

Retroviral gene transfer

We generated cells that stably overexpressed wild-type or mutant HRAS by retroviral gene transfer. Phoenix cells (5×10^6) were plated in a 10 cm dish, incubated for 24 h and then transfected with 18 μg of retroviral plasmid using Fugene6 (Roche Applied Science, Mannheim, Germany). After 48 h, the virus-containing medium was filtered through a 0.45-μm filter and supplemented with 4 μg/ml polybrene (Sigma) to collect the virus (first supernatant). Viruses were collected after an additional 24 h as before (second supernatant). BJ fibroblasts were plated at 6×10^5 cells per 10 cm dish and incubated overnight. For infections, the culture medium was replaced with the first viral supernatant and incubated at 37 °C for 8 h, after which the second viral supernatant was added. Infected cell populations were selected 40 h later, using 2 μg/ml puromycin or 200 μg/ml zeocin. The ecotropic retrovirus receptor was introduced into the BJ human fibroblasts by infecting cell populations with an amphotropic vector (pBabe-zeo-ecotropic receptor produced in Phoenix Ampho cells), allowing subsequent infection with ecotropic viruses.

RESULTS

Mutation analysis in patients with CS

Genomic sequencing analysis of 32 individuals with confirmed or suspected CS revealed four different missense mutations in 21 patients: a heterozygous 34G>A mutation (p.G12S) in 16 patients, a heterozygous 35G>C mutation (p.G12A) in three patients, a heterozygous 34G>T change (p.G12C) in one patient, and a 35G>A change (p.G12D) in one patient.

The clinical data for 21 CS mutation-positive patients are shown in Table 1. Curly and/or sparse hair (21/21), failure to thrive (21/21), coarse facial appearance (20/20), deep palmar/planter creases (20/21), soft, loose skin (18/21) and relative macrocephaly (17/21) were observed at high frequency in patients with CS, as previously reported.[1,3] Laryngomalacia (soft larynx), which has been reported in several patients with CS,[36–38] was observed in three patients. One patient had hypertension, which was also observed in a mouse model of CS.[39] One patient had glycogen storage disease type III, as previously reported by Kaji *et al.*,[40] accompanied by a p.G12S mutation. Bladder cancer was observed in one patient.

One patient (NS 223) with *HRAS* p.G12C had severe clinical manifestations of CS and was treated with pravastatin.[41] She was born at 23 weeks of gestation with extremely low birth weight (766 g, >90th percentile), even though her mother had received tocolytic therapy. Her Apgar scores were 3 and 7 at 1 and 5 min, respectively. She required mechanical ventilation. Extubation was attempted periodically beginning at day 70, but it was unsuccessful until she turned 2 years old, because of her laryngomalacia and increased mucus secretion. Hypertrophic cardiomyopathy was first observed on day 38. The patient was given propranolol and cibenzoline to control the gradual progression of hypertrophic cardiomyopathy. Cardiac arrest after extubation occurred on day 192 and the patient was successfully resuscitated. Papillomas developed at approximately 11 months of age. Erosion and itching of skin were not well controlled by topical steroids or antihistamines. Pravastatin (0.2～0.4 mg/kg/day) was administered in anticipation of its suppressive effect on RAS, beginning when she was 16 months old. Thereafter, the papillomas disappeared once and appeared again, but were less numerous than when they first appeared. The effects of pravastatin on hypertrophic cardiomyopathy were not obvious. The patient was discharged from the hospital at 2 years of age.

Analysis of mutant HRAS activation states and effects on the downstream pathway

We performed RAS activation assays to elucidate functional differences among the mutants identified in patients with CS. We transfected NIH 3T3 cells with wild-type *HRAS* or one of the nine *HRAS* mutants identified in patients with CS. We found an increase in guanosine triphosphate (GTP)-bound HRAS in all cells transfected with *HRAS* p.G12V, p.G12A, p.G12S, p.G12C, p.G12D, p.G13C, p.G13D, p.K117R and p.A146T. We did not detect any differences among the increases of GTP-bound HRAS in the cells transfected with *HRAS* p.G12V, p.G12A, p.G12S, p.G12C, p.G12D, p.G13C, p.G13D and p.K117R. The increase in the level of GTP-bound HRAS-p.A146T was milder than that of other mutants.

Next, we examined the effect of the identified mutations on the RAS pathway by studying the activation of ELK1 and c-Jun in transfected NIH 3T3 cells. ELK1 and c-Jun are the main nuclear targets of extracellular signal-regulated kinase and c-Jun N-terminal kinase, respectively. We transfected the pFR-luc trans-reporter vector, the pFA2-ELK1 or pFA2-cJun vector and the phRLnull-luc vector into NIH 3T3 cells and determined the relative luciferase activity (RLA) in each cell line. The basal RLA in cells transfected with active MEK1 or MEKK constructs showed a three-fold increase, compared with cells transfected with wild-type *HRAS* cDNA (Figure 1a). A significant increase in RLA was observed upon transfection with ELK1 and HRAS p.G12V, p.G12A, p.G12S, p.G12C, p.G12D, p.G13C, p.G13D, p.K117R and p.A146T (Figure 1b). The RLA of c-Jun was significantly increased in cells transfected with HRAS p.G12V, p.G12A, p.G12S, p.G12C, p.G12D, p.G13C and p.G13D (Figure 1c). In these assays with ELK1 and c-Jun, we observed no significant difference among RLAs in the cells transfected with *HRAS* p.G12V, p.G12A, p.G12S, p.G12C, p.G12D, p.G13C and p.G13D. These results suggest that HRAS-p.K117R and p.A146T had a weaker effect on the c-Jun N-terminal kinase pathway than the other mutants.

Cellular senescence in human fibroblasts transfected with HRAS mutants

The HRAS p.G12V mutant causes a senescence phenotype when transduced into human diploid fibroblasts. To examine the ability of the various mutants identified in patients with CS to cause senescence, we introduced wild-type or mutated *HRAS* cDNAs into human fibroblast BJ cells, using retroviral gene transfer. Figure 2a shows these cells six days after infection. Wild-type HRAS-induced cells exhibited a narrow and elongated morphology and they were not flat like senescent cells. They proliferated at levels similar to cells transfected with empty vector. In contrast, the p.G12V, p.G12A, p.G12S, p.G12C, p.G12D, p.G13C, p.G13D, p.K117R and p.A146T mutants produced cells with a senescence phenotype, exhibiting flat, enlarged and multivacuolated morphology and prominent nucleoli. Senescence

Table 1 Clinical findings and *HRAS* mutations in our CS patients

Patients	*NS71*	*NS123*	*NS125*	*NS132*	*NS137*	*NS139*	*NS156*	*NS157*	*NS167*	*NS181*	*NS198*	*NS217*
Gender	F	F	F	F	M	F	M	F	M	M	M	M
Age	9 months	11 years	17years	3 years	10 years	7 months	2 years 3 months	17 years	3 months	3 years	1 year 2 months	4 years 6 months
Paternal age at birth (years)	39	29	42	37	30	35	34	34	37	33	31	40
Maternal age at birth (years)	28	26	27	31	28	35	36	36	34	33	31	37
Growth and development												
Postnatal failure to thrive	+	+	+	+	+	+	+	+	+	+	+	+
Mental retardation	+	+	+	+	+	+	+	+	+	+	+	+
Craniofacial characteristics												
Relative macrocephaly	+	+	+	+	+	+	+	+	+	+	+	+
Coarse facial appearance	+	+	+	+	+	+	+	+	+	+	+	+
Muscloskeltal characteristics												
Short neck	+	+	+	+	+	+	+	+	–	+	–	+
Hyperextensive fingers	+	+	+	+	–	+	+	+	+	–	–	–
Tight Achilles tendon	–	+	+	+	+	–	+	–	–	–	–	+
Abnormal foot position	+	+	+	+	NA	+	NA	–	–	+	–	+
Skin characteristics												
Curly, sparse hair	+	+	+	+	+	+	+	+	+	+	Curly	+
Soft, loose skin	+	+	+	+	+	+	+	+	–	+	+	+
Deep palmer/ planter creases	+	+	+	+	+	+	+	+	+	+	+	+
Cardiac defect												
Hypertrophic cardiomyopathy	+	–	+	–	+	+	NA	+	–	+	–	–
Others	PS	–	–	–	–	–	PAC	Anomalous septum in the right atrium	VSD, arrhythmia	Atrial tachycardia	–	ASD, PSVT, PVC, CAR
Neoplasia												
Papillomata	–	–	+	–	–	–	NA	+	+	–	+	–
Other tumors		Bladder cancer							Heart neoplasia			
Others			GH deficiency		GSDIII	Chiari I, syringomyelia	Pyrolic stenosis	Congenial stridor, GH deficiency	Hypoplastic nails	Hypertention		Hydronephrosis, GER, laryngomalacia
HRAS mutation												
Nucleotide substitution	c.34G>A	c.35G>C	c.34G>A	c.34G>A	c.34G>A	c.34G>A	c.34G>A	c.34G>A	c.34G>A	c.34G>A	c.34G>A	c.34G>A
Amino acid substitution	p.G12S	p.G12A	p.G12S	p.G12S	p.G12S	p.G12S	p.G12S	p.G12S	p.G12S	p.G12S	p.G12S	p.G12S

Table 1 Continued

Patients	*NS223*	*NS231*	*NS239*	*NS248*	*NS254*	*NS263*	*NS299*	*NS318*	*NS324*	*Total*
Gender	F	F	M	M	F	M	F	F	F	
Age	6 months	5 months	18 years	5 years	2 months	1 month	3 years	1 month	1 year 6 months	
Paternal age at birth (years)	34	27	27	NA	37	35	34y	33	33	
Maternal age at birth (years)	36	27	26	30	34	36	35y	32	33	
Growth and development										
Postnatal failure to thrive	+	+	+	+	+	+	+	+	+	21/21
Mental retardation	+	+	+	+	NA	+	+	+	+	20/20
Craniofacial characteristics										
Relative macrocephaly	–	+	+	–	+	+	–	–	+	17/21
Coarse facial appearance	+	+	+	+	+	+	+	+	+	21/21
Muscloskeltal characteristics										
Short neck	–	+	NA	NA	+	+	+	–	–	14/19
Hyperextensive fingers	–	+	–	+	+	–	–	+	+	13/21
Tight Achilles tendon	+	NA	–	+	–	–	–	+	+	10/20
Abnormal foot position	–	–	NA	NA	NA	–	–	+	+	9/16
Skin characteristics										
Curly, sparse hair	+	Curly	Curly	+	+	+	Curly	+	Curly	21/21
Soft, loose skin	–	+	+	+	+	+	–	+	+	18/21
Deep palmer/planter creases	+	–	+	+	+	+	+	+	+	20/21
Cardiac defect										
Hypertrophic cardiomyopathy	+	–	+	+	+	+	+	+	+	14/20
Other	PAC	PVC	–	–	–	–	–	PAC	PAC	
Neoplasia										
Papillomata	+	–	+	–	–	–	–	–	–	6/20
Other tumors										
Others	Prabastatin administration	Laryngomalasia, hydrocephallus	GH deficiency, Arnold Chiari, scoliosis	Empty sella, GH deficiency, hypothyroidism, hypogonadism, syringomyelia		Hyperinsulinemia		Laryngomalasia seizure	Laryngomalasia	
HRAS mutation										
Nucleotide substitution	c.34G>T	c.35G>A	c.34G>A	c.34G>A	c.34G>A	c.35G>C	c.34G>A	c.35G>C	c.34G>A	
Amino acid substitution	p.G12C	p.G12D	p.G12S	p.G12S	p.G12S	p.G12A	p.G12S	p.G12A	p.G12S	

Abbreviations: –, absent; +, present; ASD, atrial septal defect; F, female; GER, gastroesophageal relfux; GH, growth hormone; GSDIII, glycogen storage disease III; M, male; NA, not available; PAC, premature atrial contraction; PS, pulmonic stenosis; PSVT, paroxysmal supraventricular tachycardia; PVC, premature ventricular contraction; VSD, ventricular septal defect.

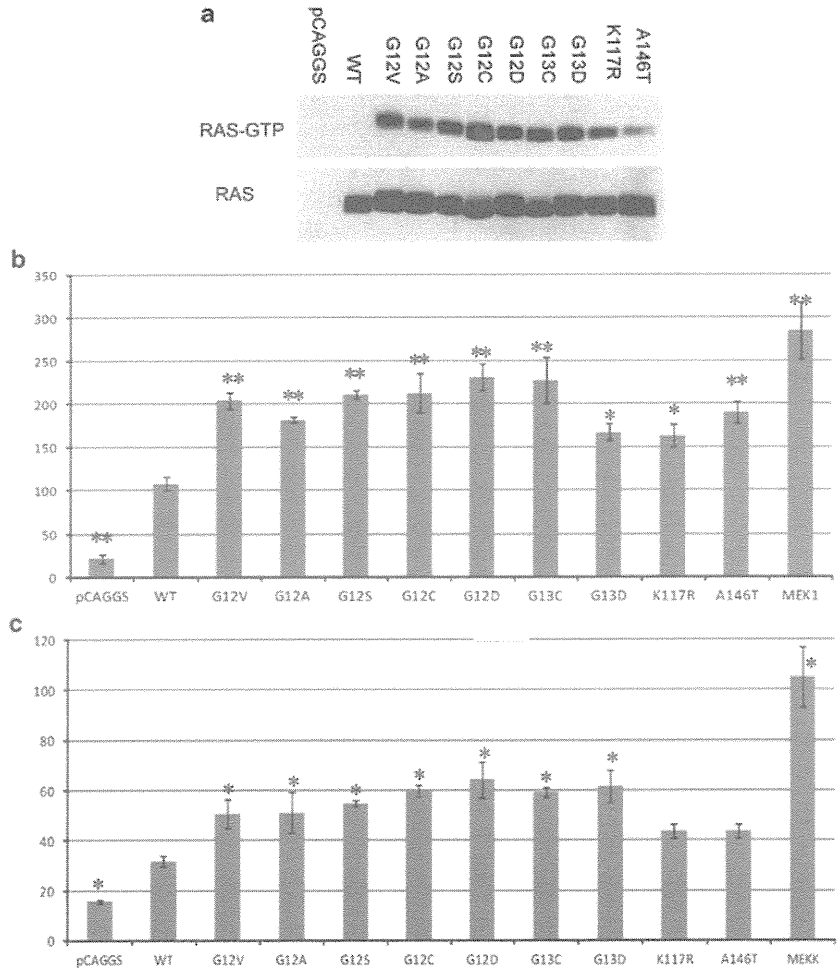

Figure 1 Functional characterization of HRAS mutants. (**a**) Ras-guanosine triphosphate (GTP) in NIH 3T3 cells transfected with wild-type or mutant HRAS constructs. HRAS protein levels were similar in NIH3T3 cells expressing each protein and were subsequently used as a loading control. (**b**, **c**) Stimulation of ELK (**b**) and c-Jun (**c**) transcription by *HRAS* mutants. The ELK-and c-Jun-GAL4 vectors and GAL4-luciferase trans-reporter vector were transiently co-transfected with various *HRAS* constructs into unstimulated NIH 3T3 cells. Relative luciferase activity (RLA) was normalized to the activity of a co-transfected control vector (phRLnull-luc) expressing *Renilla reniformis* luciferase. The results are expressed as the means and s.d. from triplicate samples. MEK1 and MEKK were used as positive controls. WT, wild type. $*P<0.05$; $**P<0.01$ compared with WT.

associated β-galactosidase staining confirmed that these cells showed cellular senescence.

Two downstream signaling pathways, p53 and Rb-p16, are activated during cellular senescence. To examine oncogene induced cellular senescence at the molecular level, we assessed senescence markers, including phosphorylated extracellular signal-regulated kinase, phosphorylated p53 and p16, in cells expressing HRAS mutant proteins (Figure 2b). As expected, phosphorylated p53 (Ser15) and p16 levels, as well as phospho-extracellular signal-regulated kinase levels, were significantly increased in the cells transfected with HRAS mutants relative to cells transfected with mock vector or wild-type HRAS. These results demonstrate that not only p.G12V, but also the other eight CS-related HRAS mutants, can cause OIS.

DISCUSSION

In this study, we identified four *HRAS* mutations in 21 patients with CS and evaluated their detailed clinical manifestations of the disease in these patients. Biochemical analyses, including a GTP binding assay and luciferase assays to detect ELK and c-Jun trans-activation, showed that there were no significant differences among the analyzed mutations in codon 12/13. The p.A146T mutant demonstrated the weakest Raf binding activity, and the p.K117R and p.A146T mutants had weaker effects on downstream c-Jun N-terminal kinase signaling than mutants in codon 12 or 13. Our results indicated that all HRAS mutants detected in CS patients were able to cause OIS.

Our study is the first to demonstrate that HRAS mutants other than p.G12V can induce senescence when they are overexpressed in human fibroblasts. The symptoms of CS seem to be caused by either hyperproliferation or hypoproliferation, coupled with growth factor resistance, which may be ascribable to DNA damage response or OIS. Postnatal cerebellar tonsillar herniation, Chiari 1 malformation,[42] deep palmar and plantar creases and papillomata may all be caused by hyperproliferation. In contrast, the poor weight gain, short stature and endocrine dysfunction observed in CS patients[43–45] might be caused by hypoproliferation. Adult brain and heart progenitor cells in a zebrafish CS model with a homozygous HRAS p.G12V mutation

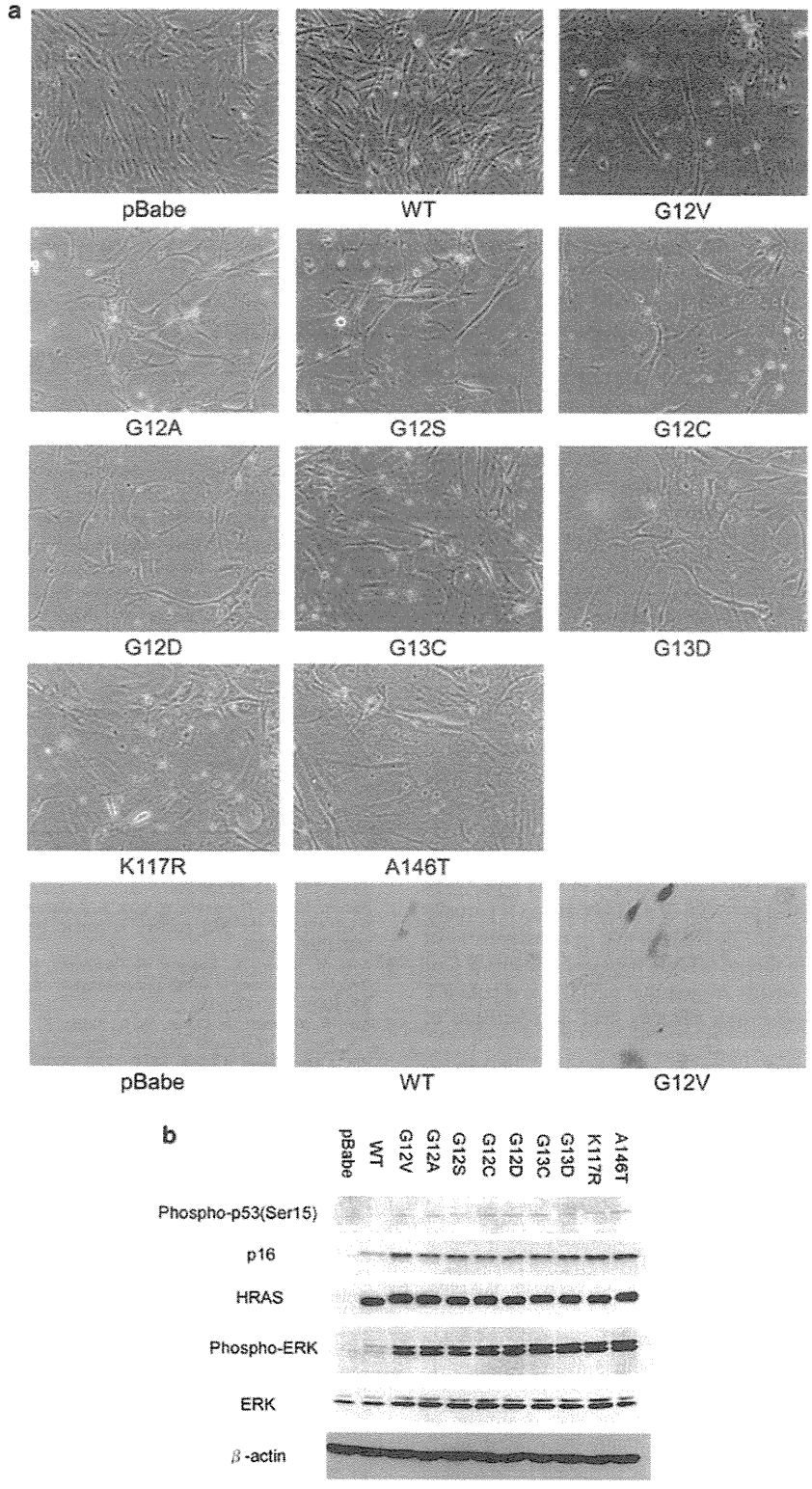

Figure 2 Effect of Costello syndrome (CS)-associated HRAS mutants on primary fibroblasts. (**a**) BJ cells transduced with retroviruses expressing wild-type or mutant HRAS. Images in the lowest tier show senescence-associated β-galactosidase staining. (**b**) Immunoblots of cellular lysates from BJ cells transduced with empty vector (pBabe) or with wild-type or mutant HRAS retroviruses.

exhibited cellular senescence, suggesting that the age-related worsening of the Costello phenotype[46] might occur, because the replicative capability of adult progenitor cells is exhausted. Osteoporosis has frequently been found in adult patients with CS,[47] suggesting that cellular senescence affects osteogenesis. However, further studies will be needed to determine whether OIS indeed contributes to the pathogenesis in patients with CS.

It has been suggested that clinical symptoms vary among patients with mutations in codon 12 or 13. In previous studies, a total of 19 CS patients have been reported to die from severe cardiomyopathy, cardiac arrhysmia, rhabdomyosarcoma, respiratory failure, multi-organ failure or sepsis. The number of fatal cases was 5/138 patients with p.G12S, 4/6 with p.G12C, 3/17 with p.G12A, 3/4 with p.G12D, 2/2 with p.G12V, 1/1 with p.G12E and 1/1 with p.E63K.[3,5–23] The mortality of patients with p.G12C or p.G12D was significantly higher than that of the patients with the more common p.G12S (P=0.026 by Fisher's exact test). Previous studies have shown that the p.G12V substitution has the highest transformative potential (p.G12V>p.G12A, p.G12S, p.G12C, p.G12D>p.G13D) and is the most frequently found mutation in human tumors.[48,49] However, our Ras activity assays and luciferase assays did not show any differences among *HRAS* codon 12/13 mutants. This may be due to the extremely high expression level of HRAS protein in our transient transfection study, which could make it difficult to detect subtle differences between mutants. Further studies will be necessary to clarify whether the high mortality in patients with p.G12C or p.G12D is due to functional differences in these mutants or due to bias because of our small sample size of patients.

Mutations at codons 117 and 146 are rare in CS and somatic cancers. Meanwhile, mutations at codons G12, G13 and Q61 have been shown to impair intrinsic and GTPase activating protein-mediated GTP hydrolysis, leading to elevated levels of cellular RAS-GTP. It has been reported that the nucleotide exchange rate of both p.K117R and p.A146V HRAS is increased, relative to wild type.[13,27,28] However, the transformational potential of p.A146V HRAS is partially activated,[27] whereas that of p.K117R-HRAS is not; its transformational activity is instead similar to that of GTPase impaired mutants.[28] Our results and those of other reports suggest that p.K117R and p.A146T have milder effects on downstream effectors than do mutations in codon 12/13.

The clinical manifestations of CS in patients with p.K117R or p.A146V mutations suggest that these alleles have distinct effects, compared with mutations in codon 12/13. Of two CS patients with a p.K117R mutation, one patient had an atypical phenotype such as microretrognatism and slightly less-pronounced plantar and palmar creases.[7] The other patient had mild craniofacial manifestations of CS.[13] One patient with the p.A146V mutation showed a mildly coarse face and did not have deep palmar creases.[6] These atypical phenotypes might be attributed to the mild effects of p.K117R or p.A146V compared with codon 12/13 mutants.

Inhibitors of the RAS/MAPK pathway could provide benefits for patients with RAS/MAPK syndromes. Statins are 3-hydroxy-3-methyl-glutaryl-CoA reductase inhibitors that result in decreased isoprenylation of RAS[50] and are now widely used for the treatment of hyperlipidemia. Statins have been used to modify the clinical manifestation of neurofibromatosis type I, which is caused by a genetic defect in a negative regulator of the RAS/MAPK pathway. Studies using mouse models of NF1 (Nf1 mice) have shown that treatment with a statin reverses the cognitive deficits of these mice.[51] A randomized control trial for neurofibromatosis type I treatment with simvastatin had a negative outcome.[52] Furthermore, statins have displayed antitumor activity in experimental tumor models, though clinical antitumor effects of statins have not been established.[53] Well-designed clinical studies will be needed to determine the effects of statins or other RAS inhibitors on manifestations of CS.

In conclusion, we identified *HRAS* mutations in 21 patients and examined the clinical manifestations of mutation-positive patients. Functional analysis revealed that CS-causing mutant HRAS proteins caused OIS in human fibroblasts. These findings may help enable more accurate prognoses for patients with *HRAS* mutations and contribute to our understanding of the mechanism underlying CS pathogenesis.

CONFLICT OF INTEREST

The authors declare no conflict of interest.

ACKNOWLEDGEMENTS

We thank the patients who participated in this study and their families and doctors, including Naoki Watanabe and Tomohiro Iwasaki, who referred the cases. We are grateful to Dr Garry Nolan of Stanford University for supplying Phoenix-Eco and Ampho cells, to Dr William C Hahn for supplying the pBabe-zeo-ecotropic receptor vector, and to Dr Jun-ichi Miyazaki of Osaka University for supplying the pCAGGS expression vector. We are also grateful to Drs Noriko Ishida and Keiko Nakayama for their technical assistance with the infection of retroviral vectors. We thank Kumi Kato and Hasumi Haba for their technical assistance. This work was supported by Grants-in-Aids for young scientists (A and S) from the Ministry of Education, Culture, Sports, Science and Technology of Japan (nos. 19689022, 21689029 and 19679005) to TN and YA, the Science and Technology Foundation of Japan Grant-in-Aid for Scientific Research to TN, and the Ministry of Health, Labour and Welfare to YM and YA.

1 Hennekam, R. C. Costello syndrome: an overview. *Am. J. Med. Genet. C. Semin. Med. Genet.* **117C,** 42–48 (2003).
2 Aoki, Y., Niihori, T., Narumi, Y., Kure, S. & Matsubara, Y. The RAS/MAPK syndromes: novel roles of the RAS pathway in human genetic disorders. *Hum. Mutat.* **29,** 992–1006 (2008).
3 Aoki, Y., Niihori, T., Kawame, H., Kurosawa, K., Ohashi, H., Tanakam, Y. *et al.* Germline mutations in HRAS proto-oncogene cause Costello syndrome. *Nat. Genet.* **37,** 1038–1040 (2005).
4 Kerr, B., Allanson, J., Delrue, M. A., Gripp, K. W., Lacombe, D., Lin, A. E. *et al.* The diagnosis of Costello syndrome: nomenclature in Ras/MAPK pathway disorders. *Am. J. Med. Genet. A* **146A,** 1218–1220 (2008).
5 Estep, A. L., Tidyman, W. E., Teitell, M. A., Cotter, P. D. & Rauen, K. A. HRAS mutations in Costello syndrome: detection of constitutional activating mutations in codon 12 and 13 and loss of wild-type allele in malignancy. *Am. J. Med. Genet. A.* **140,** 8–16 (2006).
6 Gripp, K. W., Lin, A. E., Stabley, D. L., Nicholson, L., Scott, C. I. Jr, Doyle, D. *et al.* HRAS mutation analysis in Costello syndrome: genotype and phenotype correlation. *Am. J. Med. Genet. A.* **140,** 1–7 (2006).
7 Kerr, B., Delrue, M. A., Sigaudy, S., Perveen, R., Marche, M., Burgelin, I. *et al.* Genotype-phenotype correlation in Costello syndrome: HRAS mutation analysis in 43 cases. *J. Med. Genet.* **43,** 401–405 (2006).
8 van Steensel, M. A., Vreeburg, M., Peels, C., van Ravenswaaij-Arts, C. M., Bijlsma, E., Schrander-Stumpel, C. T. *et al.* Recurring HRAS mutation G12S in Dutch patients with Costello syndrome. *Exp. Dermatol.* **15,** 731–734 (2006).
9 Gripp, K. W., Lin, A. E., Nicholson, L., Allen, W., Cramer, A., Jones, K. L. *et al.* Further delineation of the phenotype resulting from BRAF or MEK1 germline mutations helps differentiate cardio-facio-cutaneous syndrome from Costello syndrome. *Am. J. Med. Genet. A.* **143A,** 1472–1480 (2007).
10 Orstavik, K. H., Tangeraas, T., Molven, A. & Prescott, T. E. Distal phalangeal creases—a distinctive dysmorphic feature in disorders of the RAS signalling pathway? *Eur. J. Med. Genet.* **50,** 155–158 (2007).
11 Sovik, O., Schubbert, S., Houge, G., Steine, S. J., Norgard, G., Engelsen, B. *et al. De novo* HRAS and KRAS mutations in two siblings with short stature and neuro-cardio-facio-cutaneous features. *J. Med. Genet.* **44,** e84 (2007).
12 Zampino, G., Pantaleoni, F., Carta, C., Cobellis, G., Vasta, I., Neri, C. *et al.* Diversity parental germline origin, and phenotypic spectrum of *de novo* HRAS missense changes in Costello syndrome. *Hum. Mutat.* **28,** 265–272 (2007).
13 Denayer, E., Parret, A., Chmara, M., Schubbert, S., Vogels, A., Devriendt, K. *et al.* Mutation analysis in Costello syndrome: functional and structural characterization of the HRAS pLys117Arg mutation. *Hum. Mutat.* **29,** 232–239 (2008).

14 Gripp, K. W., Innes, A. M., Axelrad, M. E., Gillan, T. L., Parboosingh, J. S., Davies, C. *et al.* Costello syndrome associated with novel germline HRAS mutations: an attenuated phenotype? *Am. J. Med. Genet. A.* **146A,** 683–690 (2008).
15 Hou, J. W. Rapidly progressive scoliosis after successful treatment for osteopenia in Costello syndrome. *Am. J. Med. Genet. A.* **146,** 393–396 (2008).
16 Limongelli, G., Pacileo, G., Digilio, M. C., Calabro, P., Di Salvo, G., Rea, A. *et al.* Severe, obstructive biventricular hypertrophy in a patient with Costello syndrome: clinical impact and management. *Int. J. Cardiol.* **130,** e108–e110 (2008).
17 Schulz, A.L., Albrecht, B., Arici, C., van der Burgt, I., Buske, A., Gillessen-Kaesbach, G. *et al.* Mutation and phenotypic spectrum in patients with cardio-facio-cutaneous and Costello syndrome. *Clin. Genet.* **73,** 62–70 (2008).
18 Gremer, L., De Luca, A., Merbitz-Zahradnik, T., Dallapiccola, B., Morlot, S., Tartaglia, M. *et al.* Duplication of Glu37 in the switch I region of HRAS impairs effector/GAP binding and underlies Costello syndrome by promoting enhanced growth factor-dependent MAPK and AKT activation. *Hum. Mol. Genet.* **19,** 790–802 (2010).
19 Kuniba, H., Pooh, R.K., Sasaki, K., Shimokawa, O., Harada, N., Kondoh, T. *et al.* Prenatal diagnosis of Costello syndrome using 3D ultrasonography amniocentesis confirmation of the rare HRAS mutation G12D. *Am. J. Med. Genet. A.* **149A,** 785–787 (2009).
20 Lin, A. E., O'Brien, B., Demmer, L. A., Almeda, K. K., Blanco, C. L., Glasow, P. F. *et al.* Prenatal features of Costello syndrome: ultrasonographic findings and atrial tachycardia. *Prenat. Diagn.* **29,** 682–690 (2009).
21 Piccione, M., Piro, E., Pomponi, M. G., Matina, F., Pietrobono, R., Candela, E. *et al.* A premature infant with Costello syndrome due to a rare G13C HRAS mutation. *Am. J. Med. Genet. A.* **149A,** 487–489 (2009).
22 Sol-Church, K., Stabley, D. L., Demmer, L. A., Agbulos, A., Lin, A. E., Smoot, L. *et al.* Male-to-male transmission of Costello syndrome: G12S HRAS germline mutation inherited from a father with somatic mosaicism. *Am. J. Med. Genet. A.* **149A,** 315–321 (2009).
23 Zhang, H., Ye, J. & Gu, X. Recurring G12S mutation of HRAS in a Chinese child with Costello syndrome with high alkaline phosphatase level. *Biochem. Genet.* **47,** 868–871 (2009).
24 van der Burgt, I., Kupsky, W., Stassou, S., Nadroo, A., Barroso, C., Diem, A. *et al.* Myopathy caused by HRAS germline mutations: implications for disturbed myogenic differentiation in the presence of constitutive HRas activation. *J. Med. Genet.* **44,** 459–462 (2007).
25 McGrath, J. P., Capon, D. J., Goeddel, D. V. & Levinson, A. D. Comparative biochemical properties of normal and activated human ras p21 protein. *Nature.* **310,** 644–649 (1984).
26 Al-Mulla, F., Milner-White, E. J., Going, J. J. & Birnie, G. D. Structural differences between valine-12 and aspartate-12 Ras proteins may modify carcinoma aggression. *J. Pathol.* **187,** 433–438 (1999).
27 Feig, L. A. & Cooper, G. M. Relationship among guanine nucleotide exchange, GTP hydrolysis, and transforming potential of mutated ras proteins. *Mol. Cell. Biol.* **8,** 2472–2478 (1988).
28 Der, C. J., Weissman, B. & Macdonald, M. J. Altered guanine-nucleotide binding and H-Ras transforming and differentiating activities. *Oncogene.* **3,** 105–112 (1988).
29 Sikora, E., Arendt, T., Bennett, M. & Narita, M. Impact of cellular senescence signature on ageing research. *Ageing Res. Rev.* **10,** 146–152 (2010).
30 Serrano, M., Lin, A. W., McCurrach, M. E., Beach, D. & Lowe, S. W. Oncogenic ras provokes premature cell senescence associated with accumulation of p53 and p16INK4a. *Cell* **88,** 593–602 (1997).
31 Narita, M., Nunez, S., Heard, E., Narita, M., Lin, A. W., Hearn, S. A. *et al.* Rb-mediated heterochromatin formation and silencing of E2F target genes during cellular senescence. *Cell* **113,** 703–716 (2003).
32 Di Micco, R., Fumagalli, M., Cicalese, A., Piccinin, S., Gasparini, P., Luise, C. *et al.* Oncogene-induced senescence is a DNA damage response triggered by DNA hyper-replication. *Nature* **444,** 638–642 (2006).
33 Bartkova, J., Rezaei, N., Liontos, M., Karakaidos, P., Kletsas, D., Issaeva, N. *et al.* Oncogene-induced senescence is part of the tumorigenesis barrier imposed by DNA damage checkpoints. *Nature* **444,** 633–637 (2006).
34 Narita, M. & Lowe, S. W. Senescence comes of age. *Nat. Med.* **11,** 920–922 (2005).
35 Campisi, J. Suppressing cancer: the importance of being senescent. *Science* **309,** 886–887 (2005).
36 Kawame, H., Matsui, M., Kurosawa, K., Matsuo, M., Masuno, M., Ohashi, H. *et al.* Further delineation of the behavioral and neurologic features in Costello syndrome. *Am. J. Med. Genet. A.* **118A,** 8–14 (2003).
37 Kalfa, D., Fraisse, A. & Kreitmann, B. Medical and surgical perspectives of cardiac hypertrophy in Costello syndrome. *Cardiol. Young* **19,** 644–647 (2009).
38 Digilio, M. C., Sarkozy, A., Capolino, R., Chiarini Testa, M. B., Esposito, G., de Zorzi, A. *et al.* Costello syndrome: clinical diagnosis in the first year of life. *Eur. J. Pediatr.* **167,** 621–628 (2008).
39 Schuhmacher, A. J., Guerra, C., Sauzeau, V., Canamero, M., Bustelo, X. R. & Barbacid, M. A mouse model for Costello syndrome reveals an Ang II-mediated hypertensive condition. *J. Clin. Invest.* **118,** 2169–2179 (2008).
40 Kaji, M., Kurokawa, K., Hasegawa, T., Oguro, K., Saito, A., Fukuda, T. *et al.* A case of Costello syndrome and glycogen storage disease type III. *J. Med. Genet.* **39,** E8 (2002).
41 Omori, I., Shimizu, M. & Watanabe, T. An infant with Costello syndrome and a rare HRAS mutation (G12C). *J. Jpn. Pediatr. Soc.* **114,** 1592–1597 (2010).
42 Gripp, K. W., Hopkins, E., Doyle, D. & Dobyns, W.B. High incidence of progressive postnatal cerebellar enlargement in Costello syndrome: brain overgrowth associated with HRAS mutations as the likely cause of structural brain and spinal cord abnormalities. *Am. J. Med. Genet. A.* **152A,** 1161–1168 (2010).
43 Gregersen, N. & Viljoen, D. Costello syndrome with growth hormone deficiency and hypoglycemia: a new report and review of the endocrine associations. *Am. J. Med. Genet. A:* **129A,** 171–175 (2004).
44 Stein, R. I., Legault, L., Daneman, D., Weksberg, R. & Hamilton, J. Growth hormone deficiency in Costello syndrome. *Am. J. Med. Genet. A.* **129A,** 166–170 (2004).
45 Alexander, S., Ramadan, D., Alkhayyat, H., Al-Sharkawi, I., Backer, K. C., El-Sabban, F. *et al.* Costello syndrome and hyperinsulinemic hypoglycemia. *Am. J. Med. Genet. A.* **139,** 227–230 (2005).
46 Santoriello, C., Deflorian, G., Pezzimenti, F., Kawakami, K., Lanfrancone, L., d'Adda di Fagagna, F. *et al.* Expression of H-RASV12 in a zebrafish model of Costello syndrome causes cellular senescence in adult proliferating cells. *Dis. Model. Mech.* **2,** 56–67 (2009).
47 White, S. M., Graham, J. M. Jr, Kerr, B., Gripp, K., Weksberg, R., Cytrynbaum, C. *et al.* The adult phenotype in Costello syndrome. *Am. J. Med. Genet. A.* **136,** 128–135 (2005).
48 Seeburg, P. H., Colby, W. W., Capon, D. J., Goeddel, D. V. & Levinson, A. D. Biological properties of human c-Ha-ras1 genes mutated at codon 12. *Nature* **312,** 71–75 (1984).
49 Fasano, O., Aldrich, T., Tamanoi, F., Taparowsky, E., Furth, M. & Wigler, M. Analysis of the transforming potential of the human H-ras gene by random mutagenesis. *Proc. Natl Acad. Sci. USA* **81,** 4008–4012 (1984).
50 Jakobisiak, M. & Golab, J. Statins can modulate effectiveness of antitumor therapeutic modalities. *Med. Res. Rev.* **30,** 102–135 (2010).
51 Li, W., Cui, Y., Kushner, S. A., Brown, R. A., Jentsch, J. D., Frankland, P. W. *et al.* The HMG-CoA reductase inhibitor lovastatin reverses the learning and attention deficits in a mouse model of neurofibromatosis type 1. *Curr. Biol.* **15,** 1961–1967 (2005).
52 Krab, L. C., de Goede-Bolder, A., Aarsen, F. K., Pluijm, S. M., Bouman, M. J., van der Geest, J. N. *et al.* Effect of simvastatin on cognitive functioning in children with neurofibromatosis type 1: a randomized controlled trial. *JAMA* **300,** 287–294 (2008).
53 Dale, K. M., Coleman, C. I., Henyan, N. N., Kluger, J. & Whitem, C. M. Statins and cancer risk: a meta-analysis. *JAMA* **295,** 74–80 (2006).

Drug Metab. Pharmacokinet. 26 (5): 516–522 (2011).

Regular Article

Association between Cancer Risk and Drug-metabolizing Enzyme Gene (*CYP2A6*, *CYP2A13*, *CYP4B1*, *SULT1A1*, *GSTM1*, and *GSTT1*) Polymorphisms in Cases of Lung Cancer in Japan

Yuichiro TAMAKI[1], Tomio ARAI[2], Haruhiko SUGIMURA[3], Takamitsu SASAKI[4], Masashi HONDA[1], Yuka MUROI[1], Yoichi MATSUBARA[5], Shuichi KANNO[6], Masaaki ISHIKAWA[6], Noriyasu HIRASAWA[1] and Masahiro HIRATSUKA[1,*]

[1]*Laboratory of Pharmacotherapy of Life-Style Related Diseases, Graduate School of Pharmaceutical Sciences, Tohoku University, Sendai, Japan*

[2]*Department of Pathology, Tokyo Metropolitan Geriatric Hospital and Institute of Gerontology, Tokyo, Japan*

[3]*First Department of Pathology, Hamamatsu University School of Medicine, Hamamatsu, Japan*

[4]*Department of Environmental and Health Science, Tohoku Pharmaceutical University, Sendai, Japan*

[5]*Department of Medical Genetics, Tohoku University School of Medicine, Sendai, Japan*

[6]*Department of Clinical Pharmacotherapeutics, Tohoku Pharmaceutical University, Sendai, Japan*

Full text of this paper is available at http://www.jstage.jst.go.jp/browse/dmpk

Summary: Genetic polymorphisms of enzymes involved in the metabolism of carcinogens are suggested to modify an individual's susceptibility to lung cancer. The purpose of this study was to investigate the relationship between lung cancer cases in Japan and variant alleles of cytochrome P450 (CYP) 2A6 (*CYP2A6*4*), CYP2A13 (*CYP2A13*1-*10*), CYP4B1 (*CYP4B1*1-*7*), sulfotransferase 1A1 (*SULT1A1*2*), glutathione *S*-transferase M1 (*GSTM1* null), and glutathione *S*-transferase T1 (*GSTT1* null). We investigated the distribution of these polymorphisms in 192 lung cancer patients and in 203 age- and sex-matched cancer-free controls. The polymorphisms were analyzed using various techniques including allele-specific PCR, hybridization probe assay, multiplex PCR, denaturing high-performance liquid chromatography (DHPLC), and direct sequencing. We also investigated allele and genotype frequencies and their association with lung cancer risk, demographic factors, and smoking status. The prevalence of the *CYP2A6*4/*4* genotype in lung cancer cases was 3.6%, compared with 9.4% in the controls (adjusted OR = 0.36, 95% CI = 0.15–0.88, $P = 0.025$). In contrast, there was no association between the known *CYP2A13*, *CYP4B1*, *SULT1A1*, *GSTM1*, and *GSTT1* polymorphisms and lung cancer. These data indicate that *CYP2A6* deletions may be associated with lung cancer in the Japanese population studied.

Keywords: lung cancer; CYP2A6; CYP2A13; CYP4B1; SULT1A1; GSTM1; GSTT1; genetic polymorphism

Introduction

Lung cancer is a major cause of cancer-related death worldwide.[1)] In Japan, lung cancer is the most common cause of death in the male population and the second most common cause of death in the female population, after colon cancer. Identifying the risk factors for lung cancer development is essential to prevent this deadly disease. Environmental exposure to tobacco smoke is the primary risk factor for lung cancer.[2,3)] Tobacco smoke contains hundreds of known and probable carcinogens that are either activated or detoxified by xenobiotic metabolizing enzymes. In general, the metabolism of xenobiotics consists of phases I and II. Phase I enzymes, mainly cytochrome P450 (CYP), are typically involved in metabolic pathways involving activation of carcinogens, whereas phase II enzymes play a central role in detoxification.

Received; May 25, 2011, Accepted; June 21, 2011
J-STAGE Advance Published Date: July 26, 2011, doi:10.2133/dmpk.DMPK-11-RG-046
**To whom correspondence should be addressed:* Masahiro HIRATSUKA, Ph.D., *Laboratory of Pharmacotherapy of Life-Style Related Diseases, Graduate School of Pharmaceutical Sciences, Tohoku University, 6-3 Aoba, Aramaki, Aoba-ku, Sendai 980-8578, Japan. Tel. +81-22-717-7049, Fax. +81-22-717-7049, E-mail: mhira@m.tohoku.ac.jp*
This work was supported by a grant from the Smoking Research Foundation, Japan.

Human CYP2A6 and CYP2A13 are important phase I enzymes involved in metabolizing nicotine and the metabolic activation of tobacco-specific nitrosamines such as 4-(methylnitrosamino)-1-(3-pyridyl)-1-butanone (NNK).[4,5] CYP2A6 is mainly expressed in the human liver, whereas CYP2A13 is selectively expressed in the human respiratory tract.[5,6] To date, a large number of *CYP2A6* and *CYP2A13* genetic polymorphisms and alleles have been identified (http://www.cypalleles.ki.se/). These alleles are derived from single nucleotide polymorphisms (SNPs) in regulatory and coding regions, deletions, insertions, and conversions. *CYP2A6*4* is a major mutant allele associated with decreased metabolic activity.[7] Several studies have elucidated the role of the *CYP2A6*4* allele in tobacco dependence and lung cancer risk.[8–10] Similarly, the *CYP2A13* polymorphism 3375C>T has been correlated with a reduced risk of lung adenocarcinoma in a Chinese population.[11]

CYP4B1 is primarily an extrahepatic form of P450. CYP4B1 mRNA has been detected in the human lung and bladder.[12,13] In animals, CYP4B1 is involved in the metabolism of several xenobiotics such as 2-aminofluorene, 2-naphthylamine, and benzidine.[14,15] To date, seven variant alleles of *CYP4B1* have been identified in French Caucasian and Japanese individuals. We previously reported that the alleles *CYP4B1*2* (AT881–882del, 993G>A, 1018C>T, and 1123C>T) and *CYP4B1*3* (517C>T) are common in the Japanese population.[16] In particular, premature termination of protein synthesis by the double nucleotide deletion AT881–882del has been speculated to render the *CYP4B1*2* allele non-functional. *CYP4B1* genotypes may have an effect on the risk of bladder cancer;[17] however, it is unclear whether *CYP4B1* polymorphisms are associated with lung cancer susceptibility.

Sulfotransferases (SULTs) appear to play an important role in phase II metabolism of xenobiotics, small endogenous compounds, and procarcinogenic agents.[18,19] Some studies have shown that genetic polymorphisms of *SULT1A1* are associated with susceptibility to lung cancer.[20,21]

Glutathione *S*-transferases (GSTs) are phase II enzymes that catalyze the conjugation of reactive intermediates to soluble glutathione. Some GSTs are polymorphic, and some genetic variants, such as *GSTM1* null and *GSTT1* null, may be associated with increased susceptibility to lung cancer.[22,23] Homozygous deletions of the *GSTM1* and *GSTT1* genes are common and result in complete loss of enzyme activity.

We conducted a case-control study to examine the association between the risk of lung cancer in Japanese individuals and P450s CYP2A6 (*CYP2A6*4*), CYP2A13 (*CYP2A13*1-*10*), CYP4B1 (*CYP4B1*1-*7*), sulfotransferase 1A1 (*SULT1A1*2*), glutathione *S*-transferase M1 (*GSTM1* null), and glutathione *S*-transferase T1 (*GSTT1* null) polymorphisms. In addition, we investigated the effect of smoking status and genetic combinations on the association between lung cancer risk and genetic polymorphisms.

Materials and Methods

Subject selection: From February 1995 to July 2003, 1,536 autopsies were performed at the Department of Pathology, Tokyo Metropolitan Geriatric Medical Center, Tokyo, Japan. DNA samples from 395 of these autopsies were analyzed in this case-control study; 192 lung cancer cases and 203 cancer-free controls were sex- and age-matched. The smoking status of the individuals was retrospectively determined by reviewing medical records, and subjects were classified as smokers (including current smokers and ex-smokers) and non-smokers (individuals who have never smoked in their lifetime). Research protocols were approved by the Ethics Committees of Tokyo Metropolitan Geriatric Hospital and the Graduate School of Pharmaceutical Sciences, Tohoku University.

Genetic analysis: The presence of *CYP2A6*4* (whole gene deletion) was determined by the two-step allele-specific PCR assay described by Oscarson *et al.*[24] The first step involved amplification of a region from exon 7 to approximately 420 bp downstream of exon 9 of *CYP2A6* or the *CYP2A6/CYP2A7* hybrid from all individuals with or without the deleted *CYP2A6* gene. The reaction mixture contained approximately 30 ng genomic DNA, 0.5 μM of each primer (2AE7F, 5′-GGCCAAGATGCCCTACATG-3′; 2A6R1, 5′-GCACTTATGTTTTGTGAGACATCAGAGACAA-3′), 0.25 mM dNTPs, LA Taq polymerase (TaKaRa, Otsu, Japan), and 2× GC Buffer I (TaKaRa) in a total reaction volume of 16 μL. The thermal cycling conditions were as follows: 95°C for 1 min; followed by 30 cycles of denaturation at 95°C for 15 s, annealing at 60°C for 20 s, extension at 72°C for 3 min; and a final extension at 72°C for 7 min. The PCR product was then used as a template in the second step, in which the deleted *CYP2A6* gene was detected. PCR amplification was performed with 0.5 μL of the first PCR product, 0.25 μM forward primer (2A6E8F, 5′-CACTTCCTGAATGAG-3′, or 2A7E8F, 5′-CATTTCCTGGATGAC-3′), 0.25 μM reverse primer (2A6R2, 5′-AAAATGGGCATGAACGCCC-3′), and 2× Amplitaq Gold PCR Master Mix (Applied Biosystems, Foster City, CA, USA) in a total volume of 20 μL. Thermal cycling conditions involved an initial denaturation at 95°C for 10 min; followed by 16 cycles of denaturation at 95°C for 30 s, annealing at 56°C for 30 s, extension at 72°C for 2 min; and a final extension at 72°C for 7 min. Amplified products were analyzed by electrophoresis in 1% agarose gel. The presence of a *CYP2A*-specific 1181-bp product amplified with the 2A6E8F/2A6R2 primer pair indicated the presence of wild-type *CYP2A6* (defined as *CYP2A6 non*4* allele in this study). The product amplified from the primer pair 2A7E8F/2A6R2 indicated a *CYP2A6* deletion (*CYP2A6*4*), and the presence of the product in both reactions from one individual indicated heterozygosity.

CYP2A13 genotypes were determined by our previously described assay.[25] Long PCR was performed in the first

round to amplify exons 1–5 and 6–9 of the *CYP2A13* gene using 10–50 ng of genomic DNA and LA-Taq DNA polymerase (TaKaRa). The thermal cycling consisted of an initial denaturation at 95°C for 1 min; followed by 25 cycles of denaturation at 95°C for 15 s, annealing at 68°C or 65°C for 20 s, and extension at 72°C for 5 min; and then a final extension at 72°C for 7 min. First-round PCR products were diluted 1:500 and used as templates for the second round of amplification for all *CYP2A13* exons. The amplicons for each exon were generated using AmpliTaq Gold PCR Master Mix (Applied Biosystems). Second-round PCR comprised an initial denaturation at 95°C for 10 min; followed by 25 cycles at 95°C for 30 s, annealing at 60°C for 30 s, and extension at 72°C for 30 s; and then a final extension at 72°C for 7 min. Heteroduplexes were generated by thermal cycling under the following conditions: 95°C for 1 min, followed by 45 temperature decrements of 1.5°C/min. PCR products were analyzed with the DHPLC system WAVE (Transgenomic Inc., Omaha, NE, USA). This involved separating PCR products (5 μL) on a heated C18 reverse-phase column using 0.1 M triethylammonium acetate (TEAA) in water and 0.1 M TEAA in 25% acetonitrile at a flow rate of 0.9 mL/min. The temperature for heteroduplex separation of a heterozygous *CYP2A13* fragment was determined with the WAVE software, and the linear acetonitrile gradient was adjusted so that the retention time of the DNA peak was 3–5 min. The resultant chromatograms were compared with those of wild-type DNA, and both DNA strands were sequenced for samples in which variants were detected.

*CYP4B1*1* (wild-type), *CYP4B1*2* (AT881-882del, 993G>A, 1018C>T, and 1123C>T), *CYP4B1*3* (517C>T), *CYP4B1*5* (993G>A), *CYP4B1*6* (517C>T and 1033G>A), and *CYP4B1*7* (AT881-882del, 993G>A, and 1018C>T) were also genotyped by the hybridization probe assay described by Sasaki *et al.*[17] Analysis of the distribution of the five polymorphisms (517C>T, AT881-882del, 993G>A, 1033G>A, and 1123C>T) allowed the characterization of six different *CYP4B1* alleles.

*SULT1A1*1* (wild-type) and *SULT1A1*2* (638G>A) were genotyped by a hybridization probe assay. The PCR mixtures contained 3 mM $MgCl_2$, 0.5 μM each of the PCR primers, 0.4 μM of LC Red 640-labeled hybridization probes, 0.2 μM fluorescein isothiocyanate (FITC)-labeled hybridization probes, 1 μM LightCycler DNA Master Hybridization Mix (Roche Diagnostics Inc., Mannheim, Germany), and approximately 30 ng of genomic DNA in a final volume of 10 μL. The thermal profile consisted of 30 s of initial denaturation at 95°C, followed by 45 cycles at 95°C for 1 s, annealing at 50°C for 5 s, and extension at 72°C for 5 s. The analytical melting program involved melting the PCR products at 95°C for 30 s and at 40°C for 30 s, followed by increasing the temperature to 80°C at a ramp rate of 0.2°C/s, with continuous fluorescence data collection.

GSTM1 and *GSTT1 null* (whole gene deletion) were identified by a multiplex PCR assay described by Abdel-Rahman *et al.*[26] Genomic DNA (10–50 ng) was amplified in a 20-μL reaction mixture containing 0.25 μM of each of the *GSTM1* and *GSTT1* primers. Exon 7 of the *CYP1A1* gene was co-amplified as an internal control. Thermal cycling conditions comprised denaturation at 95°C for 10 min; 30 cycles of denaturation at 95°C for 30 s, annealing at 62°C for 30 s, and extension at 72°C for 30 s; and a final extension at 72°C for 7 min. PCR products from co-amplification of the *GSTM1*, *GSTT1*, and *CYP1A1* genes were analyzed by electrophoresis in 2% agarose gel. The *GSTM1* and *GSTT1* genes were detected by the presence or absence of a 215-bp (corresponding to *GSTM1*) or a 480-bp band (corresponding to *GSTT1*).

Statistical analysis: We evaluated the frequency distribution of patient characteristics, including sex, age, and smoking status, between the lung cancer cases and controls with the chi-squared and unpaired *t*-tests. Hardy-Weinberg equilibrium (HWE) was tested separately for each genotype in the cases and controls. The crude odds ratio (crude OR) and 95% confidence interval (95% CI) were used as estimates of the relative risk. The adjusted OR was calculated using binominal logistic regression to control for sex, age, and smoking status. A two-tailed P value < 0.05 indicated statistical significance. All statistical analyses were performed with Dr. SPSS software (Ver. 11.0.1).

Results

Cases and controls were classified according to sex, age, smoking status, and histological types of lung cancer (**Table 1**). The mean ages at the time of death were 80.3 ± 7.9 years in lung cancer patients and 80.3 ± 7.7 years in the cancer-free controls ($P = 0.991$). There were no statistically significant differences in sex distribution between the two groups (67.2% male cancer patients versus 69.0% male control patients, $P = 0.705$). More smokers were present in the cancer group compared with the control group (70.3% smokers among the cancer patients versus 51.7% smokers among the controls, $P < 0.001$). Of the 192 cancer patients, 41.7% had adenocarcinoma (AC), 24.5% had squamous cell carcinoma (SQCC), 21.4% had small-cell carcinoma (SCC), and 12.4% had other types of lung cancer.

The genotype distributions of *CYP2A6*, *CYP2A13*, *CYP4B1*, *SULT1A1*, *GSTM1*, and *GSTT1* in lung cancer cases and controls are summarized in **Table 2**. The frequency of *CYP2A6*4/*4* in cancer cases was significantly lower than that in the controls (adjusted OR = 0.36, 95% CI = 0.15–0.88, $P = 0.025$). Although the distribution of *CYP2A13*1/*2* (9.4%) and **1/*3* (3.1%) in cancer cases was lower than that in the controls (12.3% and 3.9%, respectively), there was no significant association with lung cancer risk. In addition, the *CYP4B1*, *SULT1A1*, *GSTM1*, and *GSTT1* genotypes were not associated with lung cancer risk.

Table 1. The characteristics of subjects who had lung cancer (cases) and those not having cancer (controls)

Characteristic	Cases (n = 192)	Controls (n = 203)	*P*-value
Gender, n (%)			
Male	129 (67.2)	140 (69.0)	0.705[a]
Female	63 (32.8)	63 (31.0)	
Mean age, n (SD)	80.3 (7.9)	80.3 (7.7)	0.991[b]
Smoking status, n (%)			
Non-smokers	39 (20.3)	78 (38.4)	<0.001[a]
Smokers	135 (70.3)	105 (51.7)	
No information	18 (9.4)	20 (9.9)	
Histological type			
AC	80 (41.7)		
SQCC	47 (24.5)		
SCC	41 (21.4)		
ASQC	4 (2.1)		
LCC	1 (0.5)		
Unknown	7 (3.6)		
AC + SQCC + SCC	1 (0.5)		
SQCC + SCC + ASQC	1 (0.5)		
AC + SQCC	4 (2.1)		
AC + SCC	1 (0.5)		
AC + Unknown	2 (1.0)		
SQCC + SCC	3 (1.6)		

AC, adenocarcinoma; SQCC, squamous cell carcinoma; SCC, small-cell carcinoma; ASQC, adenosquamous cell carcinoma; LCC, large cell carcinoma; SD, Standard deviation.
[a]Chi-squared test, [b]unpaired *t* test.

Table 3 summarizes the relationship between the *CYP2A6* and *CYP2A13* genotypes among lung cancer cases and controls, stratified by smoking status. There was a statistically significant association between smokers carrying *CYP2A6*4/*4* and lung cancer risk (OR = 0.32, 95% CI = 0.10–0.99, $P = 0.049$). ORs were not calculated for non-smokers carrying *CYP2A13*1/*2* and **1/*3*, as the frequency was 0 in cancer cases. There was no statistically significant association between the *CYP4B1*, *SULT1A1*, *GSTM1*, and *GSTT1* genotypes stratified by smoking status and lung cancer risk (data not shown). When stratifying by histological type, no significant association was found for any of the analyzed polymorphisms and lung cancer risk (data not shown).

Discussion

In this study, we observed that polymorphism of the *CYP2A6* gene, but not of the *CYP2A13*, *CYP4B1*, *SULT1A1*, *GSTM1*, or *GSTT1* genes, was associated with decreased risk of lung cancer in the Japanese population studied.

Defective *CYP2A6* alleles have been associated with both increased and decreased risks of lung cancer in different ethnic groups. A Chinese lung cancer study suggested that the presence of the defective allele *CYP2A6*4* increases lung cancer risk.[10] In contrast, a Japanese lung cancer study suggested that the presence of the *CYP2A6*4* allele decreases the risk of lung cancer.[9] The results of our study were consistent with the latter study. CYP2A6 is responsible for the metabolic activation of NNK, one of the components of tobacco smoke. Reducing the production of ultimate carcinogens may lead to decreased DNA damage and reduced cancer development. This hypothesis was supported by a statistically significant association between smokers carrying *CYP2A6*4/*4* and lung cancer risk.

To the best of our knowledge, this is the first case-control study evaluating the relationship between *CYP2A13* genetic polymorphism and lung cancer risk in the Japanese population. CYP2A13 is highly active in the metabolic activation of several carcinogens. Thus, we speculated that reduction in enzymatic activity observed in the *CYP2A13*2* (74G>A and 3375C>T) allelic variant could provide some protection against xenobiotic toxicity. Wang *et al.* reported that Chinese individuals carrying the variant *CYP2A13* allele (3375CT or TT) have a reduced risk of lung adenocarcinoma in relation to light tobacco smoking, but protection against lung squamous cell carcinoma was not observed.[11] Timofeeva *et al.* found no significant association between *CYP2A13* polymorphisms and lung cancer risk in Caucasian patients.[27] We also did not find significant association between the variant *CYP2A13* allele and lung cancer. Interestingly, none of the non-smokers with lung cancer had the CYP2A13*2 or *3 alleles (**Table 3**). In non-smoking individuals with low carcinogenic activity caused by *CYP2A13* polymorphisms, the risk of lung cancer in the population may be much lower than that in smokers with CYP2A13 wild-type genotypes.

The effect of *CYP4B1* polymorphisms on susceptibility of lung cancer has not previously been investigated. Our study is the first to provide evidence that *CYP4B1* polymorphisms may not be associated with lung cancer risk. Our previous study indicated that *CYP4B1* genotypes may affect bladder cancer risk.[17] Thus, the effect of the *CYP4B1* polymorphism may differ among human organs with respect to cancer development.

Since SULT1A1 catalyzes the sulfation of numerous carcinogenic and mutagenic compounds such as heterocyclic and aromatic amines and polycyclic aromatic hydrocarbons, it was suggested that the reduction in enzymatic activity observed in *SULT1A1*2* could affect the risk of lung cancer; however, the association between *SULT1A1*2* and lung cancer risk was not statistically significant in this study. Nevertheless, Liang *et al.* conducted a study on 805 individuals with cancer and 809 control subjects in China, and demonstrated that the lung cancer risk was elevated among individuals with the *SULT1A1*2* allele.[21] The reason for the discrepancy between our results and Liang's is unknown but may be related to differences in ethnicity, sample size, or environmental carcinogen exposure.

Table 2. Genotype and allele frequencies of *CYP2A6*, *CYP2A13*, *CYP4B1*, *SULT1A1*, *GSTM1*, and *GSTT1* polymorphisms among cases and controls and their association with lung cancer

Genotypes	Cases, n (%)	Controls, n (%)	Crude OR[a] (95% CI)	Adjusted OR[b] (95% CI)
CYP2A6				
*non*4/non*4*	122 (63.5)	118 (58.1)	1.00	1.00
*non*4/*4*	63 (32.8)	66 (32.5)	0.92 (0.60–1.42)	0.93 (0.61–1.43)
**4/*4*	7 (3.6)	19 (9.4)	0.36 (0.14–0.88)[†]	0.36 (0.15–0.88)[†]
Alleles				
*non*4*	307 (79.9)	302 (74.4)	1.00	
**4*	77 (20.1)	104 (25.6)	0.73 (0.52–1.02)	
CYP2A13				
**1/*1*	163 (84.9)	166 (81.8)	1.00	1.00
**1/*2*	18 (9.4)	25 (12.3)	0.73 (0.39–1.40)	0.75 (0.39–1.44)
**1/*3*	6 (3.1)	8 (3.9)	0.76 (0.26–2.25)	0.77 (0.26–2.27)
Rare genotypes[c]	5 (2.6)	4 (2.0)	—	—
Alleles				
**1*	355 (92.4)	369 (90.9)	1.00	
**2*	18 (4.7)	25 (6.2)	0.75 (0.40–1.40)	
**3*	6 (1.6)	8 (2.0)	0.78 (0.27–2.27)	
CYP4B1				
**1/*1*	52 (27.1)	48 (23.6)	1.00	1.00
**1/*2*	67 (34.9)	61 (30.0)	1.01 (0.60–1.71)	1.00 (0.59–1.70)
**1/*3*	23 (12.0)	32 (15.8)	0.66 (0.34–1.29)	0.65 (0.33–1.27)
**2/*2*	19 (9.9)	20 (9.9)	0.88 (0.42–1.84)	0.88 (0.42–1.84)
**2/*3*	14 (7.3)	16 (7.9)	0.81 (0.36–1.83)	0.80 (0.35–1.81)
**3/*3*	7 (3.6)	7 (3.6)	0.92 (0.30–2.83)	1.00 (0.32–3.14)
Rare genotypes[d]	10 (5.2)	19 (9.4)	—	—
Alleles				
**1*	200 (52.1)	202 (49.8)	1.00	
**2*	122 (31.8)	121 (29.8)	1.02 (0.74–1.40)	
**3*	52 (13.5)	64 (15.8)	0.82 (0.54–1.24)	
SULT1A1				
**1/*1*	120 (62.5)	132 (65.0)	1.00	1.00
**1/*2*	70 (36.5)	68 (33.5)	1.13 (0.75–1.72)	1.12 (0.74–1.70)
**2/*2*	2 (1.0)	3 (1.5)	0.73 (0.12–4.46)	0.76 (0.12–4.71)
Alleles				
**1*	310 (80.7)	332 (81.8)	1.00	
**2*	74 (19.3)	74 (18.2)	1.07 (0.75–1.53)	
GSTM1				
Present	106 (55.2)	101 (49.8)	1.00	1.00
Null	86 (44.8)	102 (50.2)	0.80 (0.54–1.19)	0.80 (0.54–1.20)
GSTT1				
Present	95 (49.5)	99 (48.8)	1.00	1.00
Null	97 (50.5)	104 (51.2)	0.97 (0.66–1.44)	0.97 (0.65–1.44)

OR, odds ratio; CI, confidence interval.
[†]$P < 0.05$ (vs. *CYP2A6 non*4/non*4*).
[a]Chi-squared test. [b]Binominal logistic regression analysis adjusted by sex, age, and smoking status.
[c]Rare genotypes included: *CYP2A13*1/*4*, *CYP2A13*1/*5*, *CYP2A13*1/*7*, and *CYP2A13*1*10*.[25]
[d]Rare genotypes included: *CYP4B1*1/*5*, *CYP4B1*1/*6*, *CYP4B1*1/*7*, *CYP4B1*2/*5*, *CYP4B1*2/*6*, *CYP4B1*2/*7*, and *CYP4B1*3/*7*.

Table 3. Effect of *CYP2A6* and *CYP2A13* genotypes by smoking status on lung cancer risk

Genotypes	Smokers			Non-smokers		
	Cases/controls	Adjusted OR[a] (95% CI)	*P*-value	Cases/controls	Adjusted OR[a] (95% CI)	*P*-value
CYP2A6						
non*4/non*4	87/52	1.00		22/53	1.00	
non*4/*4	43/43	0.61 (0.35–1.05)	0.074	15/18	2.35 (0.96–5.72)	0.060
*4/*4	5/10	0.32 (0.10–0.99)	0.049	2/7	0.74 (0.14–4.01)	0.724
CYP2A13						
*1/*1	109/80	1.00		38/69	1.00	
*1/*2	17/19	0.68 (0.33–1.40)	0.293	0/5	—	—
*1/*3	5/3	1.51 (0.35–6.58)	0.585	0/3	—	—

OR, odds ratio; CI, confidence interval.
[a]Binominal logistic regression analysis adjusted by sex and age.

In the present study, there was no statistically significant association between either the *GSTM1* or *GSTT1* genotype and lung cancer risk in the Japanese subjects studied. To-Figueras *et al.* reported that 14.4% of their cancer patients possessed homozygous deletion of both *GSTT1* and *GSTM1* (12.5% among healthy smokers),[28] suggesting no potentiation between null genotypes for lung cancer risk, which is in agreement with our results. In contrast, Pinarbasi *et al.*[23] and Kihara *et al.*[22] reported that *GSTM1* null genotypes were associated with lung cancer risk in a Turkish population and in male Japanese smokers, respectively. These conflicting results, including ours, may be caused by some confounding factors such as ethnicity, selection of control group, characterization of cases, sample size, gene-gene and gene-environment interactions, and second-hand smoke conditions.

In conclusion, these results indicate that the *CYP2A6*4/*4* genotypes, but not the *CYP2A13*, *CYP4B1*, *SULT1A1*, *GSTM1*, and *GSTT1* gene polymorphisms, were associated with decreased risk of lung cancer in the Japanese population studied. However, there is an element of chance in the results in the present study because the sample size was relatively small. Therefore, further studies with larger sample sizes will be required to confirm the present findings.

Acknowledgment: We thank the Biomedical Research Core of Tohoku University Graduate School of Medicine for technical support.

References

1) Greenlee, R. T., Murray, T., Bolden, S. and Wingo, P. A.: Cancer statistics, 2000. *CA Cancer J. Clin.*, **50**: 7–33 (2000).
2) Petrauskaitė, R., Pershagen, G. and Gurevicius, R.: Lung cancer near an industrial site in Lithuania with major emissions of airway irritants. *Int. J. Cancer*, **99**: 106–111 (2002).
3) Stellman, S. D., Takezaki, T., Wang, L., Chen, Y., Citron, M. L., Djordjevic, M. V., Harlap, S., Muscat, J. E., Neugut, A. I., Wynder, E. L., Ogawa, H., Tajima, K. and Aoki, K.: Smoking and lung cancer risk in American and Japanese men: an international case-control study. *Cancer Epidemiol. Biomarkers Prev.*, **10**: 1193–1199 (2001).
4) Bao, Z., He, X. Y., Ding, X., Prabhu, S. and Hong, J. Y.: Metabolism of nicotine and cotinine by human cytochrome P450 2A13. *Drug Metab. Dispos.*, **33**: 258–261 (2005).
5) Su, T., Bao, Z., Zhang, Q. Y., Smith, T. J., Hong, J. Y. and Ding, X.: Human cytochrome P450 CYP2A13: predominant expression in the respiratory tract and its high efficiency metabolic activation of a tobacco-specific carcinogen, 4-(methylnitrosamino)-1-(3-pyridyl)-1-butanone. *Cancer Res.*, **60**: 5074–5079 (2000).
6) Koskela, S., Hakkola, J., Hukkanen, J., Pelkonen, O., Sorri, M., Saranen, A., Anttila, S., Fernandez-Salguero, P., Gonzalez, F. and Raunio, H.: Expression of CYP2A genes in human liver and extrahepatic tissues. *Biochem. Pharmacol.*, **57**: 1407–1413 (1999).
7) Nunoya, K., Yokoi, T., Kimura, K., Inoue, K., Kodama, T., Funayama, M., Nagashima, K., Funae, Y., Green, C., Kinoshita, M. and Kamataki, T.: A new deleted allele in the human cytochrome P450 2A6 (CYP2A6) gene found in individuals showing poor metabolic capacity to coumarin and (+)-cis-3,5-dimethyl-2-(3-pyridyl)thiazolidin-4-one hydrochloride (SM-12502). *Pharmacogenetics*, **8**: 239–250 (1998).
8) Ariyoshi, N., Miyamoto, M., Umetsu, Y., Kunitoh, H., Dosaka-Akita, H., Sawamura, Y., Yokota, J., Nemoto, N., Sato, K. and Kamataki, T.: Genetic polymorphism of CYP2A6 gene and tobacco-induced lung cancer risk in male smokers. *Cancer Epidemiol. Biomarkers Prev.*, **11**: 890–894 (2002).
9) Fujieda, M., Yamazaki, H., Saito, T., Kiyotani, K., Gyamfi, M. A., Sakurai, M., Dosaka-Akita, H., Sawamura, Y., Yokota, J., Kunitoh, H. and Kamataki, T.: Evaluation of CYP2A6 genetic polymorphisms as determinants of smoking behavior and tobacco-related lung cancer risk in male Japanese smokers. *Carcinogenesis*, **25**: 2451–2458 (2004).
10) Tan, W., Chen, G. F., Xing, D. Y., Song, C. Y., Kadlubar, F. F. and Lin, D. X.: Frequency of CYP2A6 gene deletion and its relation to risk of lung and esophageal cancer in the Chinese population. *Int. J. Cancer*, **95**: 96–101 (2001).
11) Wang, H., Tan, W., Hao, B., Miao, X., Zhou, G., He, F. and Lin, D.: Substantial reduction in risk of lung adenocarcinoma associated with genetic polymorphism in CYP2A13, the most active cytochrome P450 for the metabolic activation of tobacco-specific carcinogen NNK. *Cancer Res.*, **63**: 8057–8061 (2003).
12) Choudhary, D., Jansson, I., Stoilov, I., Sarfarazi, M. and Schenkman, J. B.: Expression patterns of mouse and human CYP orthologs (families 1-4) during development and in different adult tissues. *Arch. Biochem. Biophys.*, **436**: 50–61 (2005).
13) Imaoka, S., Yoneda, Y., Sugimoto, T., Hiroi, T., Yamamoto, K., Nakatani, T. and Funae, Y.: CYP4B1 is a possible risk factor for

bladder cancer in humans. *Biochem. Biophys. Res. Commun.*, **277**: 776–780 (2000).
14) Imaoka, S., Yoneda, Y., Matsuda, T., Degawa, M., Fukushima, S. and Funae, Y.: Mutagenic activation of urinary bladder carcinogens by CYP4B1 and the presence of CYP4B1 in bladder mucosa. *Biochem. Pharmacol.*, **54**: 677–683 (1997).
15) Vanderslice, R. R., Boyd, J. A., Eling, T. E. and Philpot, R. M.: The cytochrome P-450 monooxygenase system of rabbit bladder mucosa: enzyme components and isozyme 5-dependent metabolism of 2-aminofluorene. *Cancer Res.*, **45**: 5851–5858 (1985).
16) Hiratsuka, M., Nozawa, H., Konno, Y., Saito, T., Konno, S. and Mizugaki, M.: Human CYP4B1 gene in the Japanese population analyzed by denaturing HPLC. *Drug Metab. Pharmacokinet.*, **19**: 114–119 (2004).
17) Sasaki, T., Horikawa, M., Orikasa, K., Sato, M., Arai, Y., Mitachi, Y., Mizugaki, M., Ishikawa, M. and Hiratsuka, M.: Possible relationship between the risk of Japanese bladder cancer cases and the CYP4B1 genotype. *Jpn. J. Clin. Oncol.*, **38**: 634–640 (2008).
18) Falany, C. N.: Enzymology of human cytosolic sulfotransferases. *FASEB J.*, **11**: 206–216 (1997).
19) Richard, K., Hume, R., Kaptein, E., Stanley, E. L., Visser, T. J. and Coughtrie, M. W.: Sulfation of thyroid hormone and dopamine during human development: ontogeny of phenol sulfotransferases and arylsulfatase in liver, lung, and brain. *J. Clin. Endocrinol. Metab.*, **86**: 2734–2742 (2001).
20) Arslan, S., Silig, Y. and Pinarbasi, H.: An investigation of the relationship between SULT1A1 Arg(213)His polymorphism and lung cancer susceptibility in a Turkish population. *Cell Biochem. Funct.*, **27**: 211–215 (2009).
21) Liang, G., Miao, X., Zhou, Y., Tan, W. and Lin, D.: A functional polymorphism in the SULT1A1 gene (G638A) is associated with risk of lung cancer in relation to tobacco smoking. *Carcinogenesis*, **25**: 773–778 (2004).
22) Kihara, M. and Noda, K.: Risk of smoking for squamous and small cell carcinomas of the lung modulated by combinations of CYP1A1 and GSTM1 gene polymorphisms in a Japanese population. *Carcinogenesis*, **16**: 2331–2336 (1995).
23) Pinarbasi, H., Silig, Y., Cetinkaya, O., Seyfikli, Z. and Pinarbasi, E.: Strong association between the GSTM1-null genotype and lung cancer in a Turkish population. *Cancer Genet. Cytogenet.*, **146**: 125–129 (2003).
24) Oscarson, M., McLellan, R. A., Gullsten, H., Yue, Q. Y., Lang, M. A., Bernal, M. L., Sinues, B., Hirvonen, A., Raunio, H., Pelkonen, O. and Ingelman-Sundberg, M.: Characterisation and PCR-based detection of a CYP2A6 gene deletion found at a high frequency in a Chinese population. *FEBS Lett.*, **448**: 105–110 (1999).
25) Tamaki, Y., Honda, M., Muroi, Y., Arai, T., Sugimura, H., Matsubara, Y., Kanno, S., Ishikawa, M., Hirasawa, N. and Hiratsuka, M.: Novel single nucleotide polymorphism of the CYP2A13 gene in Japanese individuals. *Drug Metab. Pharmacokinet.*, in press (2011).
26) Abdel-Rahman, S. Z., el-Zein, R. A., Anwar, W. A. and Au, W. W.: A multiplex PCR procedure for polymorphic analysis of GSTM1 and GSTT1 genes in population studies. *Cancer Lett.*, **107**: 229–233 (1996).
27) Timofeeva, M. N., Kropp, S., Sauter, W., Beckmann, L., Rosenberger, A., Illig, T., Jager, B., Mittelstrass, K., Dienemann, H., Bartsch, H., Bickeboller, H., Chang-Claude, J. C., Risch, A. and Wichmann, H. E.: CYP450 polymorphisms as risk factors for early-onset lung cancer: gender-specific differences. *Carcinogenesis*, **30**: 1161–1169 (2009).
28) To-Figueras, J., Gene, M., Gomez-Catalan, J., Galan, M. C., Fuentes, M., Ramon, J. M., Rodamilans, M., Huguet, E. and Corbella, J.: Glutathione S-transferase M1 (GSTM1) and T1 (GSTT1) polymorphisms and lung cancer risk among Northwestern Mediterraneans. *Carcinogenesis*, **18**: 1529–1533 (1997).

0090-9556/11/3910-1860–1865$25.00
DRUG METABOLISM AND DISPOSITION

DMD 39:1860–1865, 2011

Vol. 39, No. 10
40352/3717294
Printed in U.S.A.

Functional Characterization of CYP2B6 Allelic Variants in Demethylation of Antimalarial Artemether

Masashi Honda, Yuka Muroi, Yuichiro Tamaki, Daisuke Saigusa, Naoto Suzuki, Yoshihisa Tomioka, Yoichi Matsubara, Akifumi Oda, Noriyasu Hirasawa, and Masahiro Hiratsuka

Laboratory of Pharmacotherapy of Life-Style Related Diseases (M.H., Y.Mu., Y.Ta., N.H., M.H.) and Laboratory of Oncology, Pharmacy Practice and Sciences, Graduate School of Pharmaceutical Sciences, Tohoku University, Sendai, Japan (D.S., N.S., Y.To.); Department of Medical Genetics, Tohoku University School of Medicine, Sendai, Japan (Y.Ma.); and Faculty of Pharmaceutical Sciences, Tohoku Pharmaceutical University, Sendai, Japan (A.O.)

Received May 5, 2011; accepted July 11, 2011

ABSTRACT:

Artemether (AM) is one of the most effective antimalarial drugs. The elimination half-life of AM is very short, and it shows large interindividual variability in pharmacokinetic parameters. The aim of this study was to identify cytochrome P450 (P450) isozymes responsible for the demethylation of AM and to evaluate functional differences between 26 CYP2B6 allelic variants in vitro. Of 14 recombinant P450s examined in this study, CYP2B6 and CYP3A4 were primarily responsible for production of the desmethyl metabolite dihydroartemisinin. The intrinsic clearance (V_{max}/K_m) of CYP2B6 was 6-fold higher than that of CYP3A4. AM demethylation activity was correlated with CYP2B6 protein levels (P = 0.004); however, it was not correlated with CYP3A4 protein levels (P = 0.27) in human liver microsomes. Wild-type CYP2B6.1 and 25 CYP2B6 allelic variants (CYP2B6.2-CYP2B6.21 and CYP2B6.23-CYP2B6.27) were heterologously expressed in COS-7 cells. In vitro analysis revealed no enzymatic activity in 5 variants (CYP2B6.8, CYP2B6.12, CYP2B6.18, CYP2B6.21, and CYP2B6.24), lower activity in 7 variants (CYP2B6.10, CYP2B6.11, CYP2B6.14, CYP2B6.15, CYP2B6.16, CYP2B6.20, and CYP2B6.27), and higher activity in 4 variants (CYP2B6.2, CYP2B6.4, CYP2B6.6, and CYP2B6.19), compared with that of wild-type CYP2B6.1. In kinetic analysis, 3 variants (CYP2B6.2, CYP2B6.4, and CYP2B6.6) exhibited significantly higher V_{max}, and 3 variants (CYP2B6.14, CYP2B6.20 and CYP2B6.27) exhibited significantly lower V_{max} compared with that of CYP2B6.1. This functional analysis of CYP2B6 variants could provide useful information for individualization of antimalarial drug therapy.

Introduction

Malaria is a very serious problem in many countries, and there are more than 200 million cases that result in approximately 1 million deaths worldwide each year (World Health Organization, World Malaria Report 2009, http://www.who.int/malaria/world_malaria_report_2009/en/index.html). The management of malaria has traditionally relied on monotherapy with quinolines such as quinine, mefloquine, and chloroquine. However, the widespread and excessive use of these agents has resulted in drug resistance (Wernsdorfer, 1991; Price and Nosten, 2001; Le Bras and Durand, 2003). In several studies, artemisinins, unique sesquiterpene lactone endoperoxides, have been used in areas with multidrug-resistant *Plasmodium falciparum* malaria (Woodrow et al., 2005; Gautam et al., 2009; World Health Organization, 2010).

This work was supported by the Japan Society for the Promotion of Science [KAKENHI 20590154] and in part by the Smoking Research Foundation.

Article, publication date, and citation information can be found at http://dmd.aspetjournals.org.

doi:10.1124/dmd.111.040352.

Artemisinin is a natural antimalarial agent derived from the Chinese medicinal plant *Artemisia annua* (Klayman, 1985). The artemisinin derivative artemether (AM) is the most effective antimalarial drug. AM has a fast onset of action, therapeutic efficacy against multidrug-resistant malaria, and few side effects, although neurotoxicity has been observed in experimental mammals (Hien and White, 1993; Brewer et al., 1994). AM is mainly converted to dihydroartemisinin (DHA) (Fig. 1), a desmethyl metabolite that contributes to the majority of the antimalarial activity. The conversion of AM to DHA is catalyzed by cytochrome P450 (P450) (van Agtmael et al., 1999b,c; Navaratnam et al., 2000). However, the elimination half-life of AM is very short, and it shows large interindividual variability in pharmacokinetic parameters (Na Bangchang et al., 1994; Mordi et al., 1997; van Agtmael et al., 1999a; Lefèvre et al., 2002; Ali et al., 2010; Mwesigwa et al., 2010).

The P450 isozymes CYP2B6 and CYP3A4 are thought to catalyze AM demethylation (Navaratnam et al., 2000). In contrast, it has been reported that CYP2D6 and CYP2C19 make no major contribution to this reaction (van Agtmael et al., 1998), and the role of other P450s remains unclear. CYP2B6 plays a major role in the biotransformation of several therapeutically important drugs, including cyclophosph-

ABBREVIATIONS: AM, artemether; DHA, dihydroartemisinin; P450, cytochrome P450; ART, artemisinin; LC, liquid chromatography; MS/MS, tandem mass spectrometry.

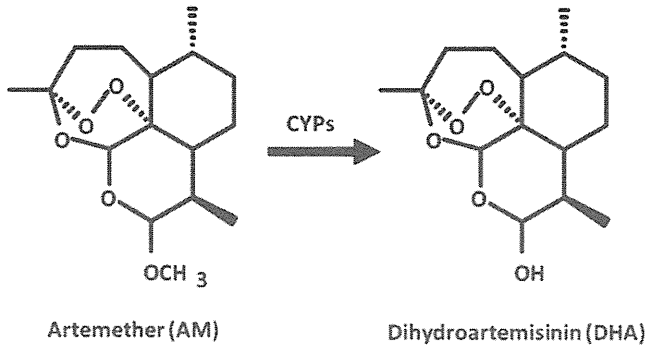

FIG. 1. Metabolic pathway of artemether to dihydroartemisinin by P450 enzymes.

amide, bupropion, selegiline, efavirenz, nevirapine, and methadone (Roy et al., 1999; Hesse et al., 2000; Hidestrand et al., 2001; Salonen et al., 2003). Many genetic polymorphisms in the *CYP2B6* gene have been reported, and these are thought to be responsible for interindividual and interethnic differences in responses to CYP2B6 substrate drugs [Zanger et al., 2007; Human Cytochrome P450 (CYP) Allele Nomenclature Committee, 2008; Mo et al., 2009]. In the case of chemotherapy using cyclophosphamide, the increasing enzymatic activity of CYP2B6 variants can be associated with the increased blood concentration of the active metabolite of the drug, resulting in a heightened risk of side effects (Xie et al., 2003, 2006; Nakajima et al., 2007).

Several functional analyses of CYP2B6 variant proteins, using an in vitro expression system, have been reported. Watanabe et al. (2010) characterized the functional relevance of many CYP2B6 variants, including CYP2B6.1 to CYP2B6.28, using 7-ethoxy-4-trifluoromethylcoumarin and selegiline as substrates, and reported that CYP2B6.8, CYP2B6.11, CYP2B6.12, CYP2B6.13, CYP2B6.15, CYP2B6.18, CYP2B6.21, CYP2B6.24, and CYP2B6.28 were inactive with regard to these compounds. These results were consistent with those of a number of in vitro studies using bupropion as a substrate. In contrast, CYP2B6.16, CYP2B6.19, and CYP2B6.27 exhibited activity toward 7-ethoxy-4-trifluoromethylcoumarin and inability to detect selegiline metabolism. Several researchers have reported that these CYP2B6 variants exhibited decreased protein expression/activity when bupropion was used as the CYP2B6 substrate (Lang et al., 2004; Klein et al., 2005; Wang et al., 2006; Rotger et al., 2007). These results suggest that some allelic variants of CYP2B6 are associated with a substrate-dependent decrease in the catalytic properties of the enzyme. To date, there have been no reports of functional characterization of CYP2B6 variants in relation to AM demethylation activity.

In this study, we performed an in vitro analysis of 14 P450s (CYP1A1, CYP1A2, CYP1B1, CYP2A6, CYP2B6, CYP2C8, CYP2C9, CYP2C19, CYP2D6, CYP2E1, CYP2J2, CYP3A4, CYP3A5, and CYP4A11) to identify isoforms responsible for AM demethylation and evaluated functional differences among 26 CYP2B6 allelic variants (Fig. 2).

Materials and Methods

Chemicals. AM, DHA, and artemisinin (ART) were purchased from Tokyo Chemical Industry Corporation (Tokyo, Japan). Recombinant CYP1A1, CYP2A6, CYP2B6, CYP2C8, CYP2D6, CYP2J2, and CYP4A11 Supersomes were purchased from BD Biosciences (Woburn, MA). CYP1A2, CYP2C9, CYP2E1, CYP3A4, and CYP3A5 Baculosomes were purchased from Invitrogen (Carlsbad, CA). NADPH was obtained from Oriental Yeast (Tokyo, Japan). Protease Inhibitor Cocktail Set III was purchased from Merck Chemicals (Darmstadt, Germany). Methanol (CH_3OH) and acetonitrile (CH_3CN) of LC-mass spectrometry grade were obtained from Kanto Chemical (Tokyo, Japan). Ammonium formate ($HCOONH_4$) and formic acid (HCOOH) of LC-mass spectrometry grade were obtained from Wako Pure Chemical Industries (Tokyo, Japan).

DHA stock solution (5 mM) was prepared in CH_3CN/H_2O [50:50 (v/v)], and working solutions (1.0, 2.0, 5.0, 10, 25, 50, 100, and 200 μM) were prepared from the stock solution. These solutions were further diluted in 50 mM potassium phosphate buffer, pH 7.4, and the final calibration curves were obtained with 0.1, 0.2, 0.5, 1.0, 2.5, 5.0, 10, and 20 μM solutions. Working solutions (100 μl) were prepared in 1.5-ml plastic tubes, and 100 μl of CH_3OH, 5 μl of internal standard (ART at 100 μM), and 100 μl of H_2O were

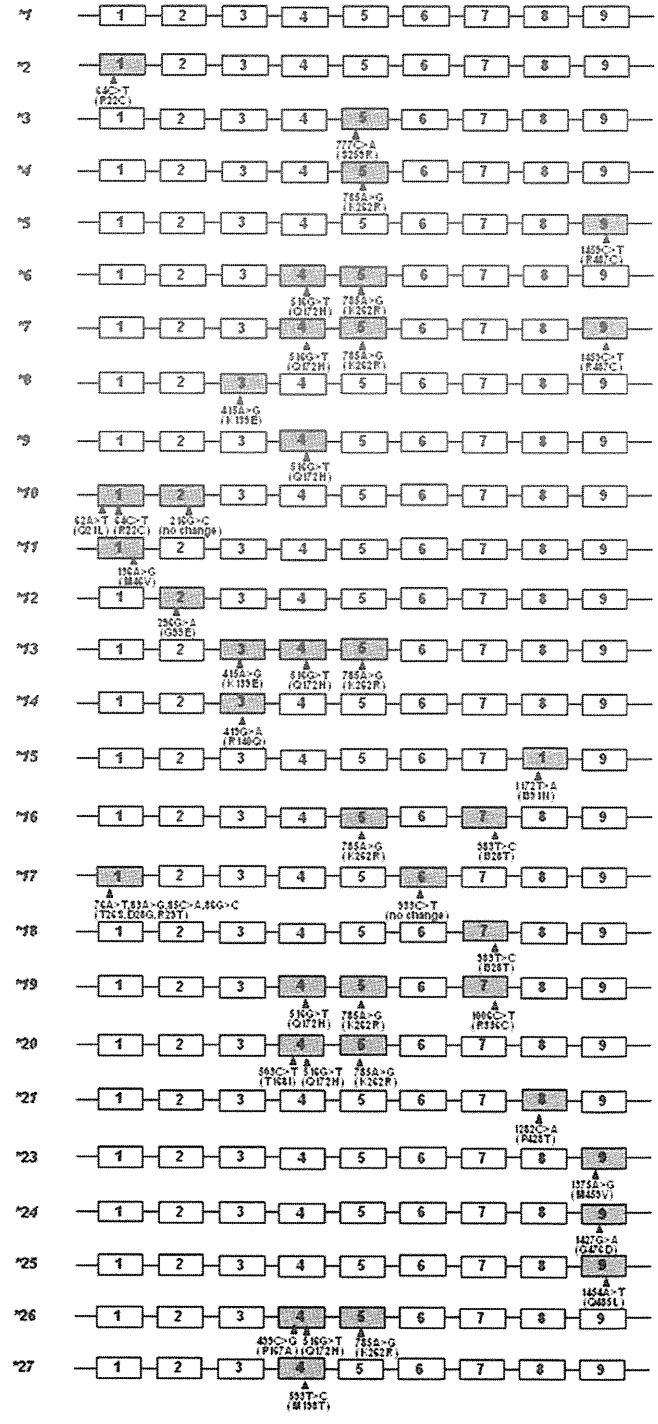

FIG. 2. Structures of CYP2B6 alleles characterized in this study. The nine exons are indicated by numbered boxes. Some promoter and intronic polymorphisms are not shown.

added. The resulting mixture was vortexed. After centrifugation at 12,000*g* for 10 min, 80 μl of the supernatant was transferred to a new plastic tube and passed through a filter (pore size: 0.2 μm; YMC Co., Ltd., Kyoto, Japan). Subsequently, 10 μl of the filtered solution was injected into the liquid chromatography-tandem mass spectrometry (LC-MS/MS) system for analysis. All peaks were integrated automatically by Xcalibur software (Thermo Fisher Scientific, Waltham, MA). Levels of DHA were calculated from the calibration curves by the ratios of their peak areas to that of ART. An eight-point calibration curve was plotted for DHA concentration (0.1, 0.2, 0.5, 1.0, 2.5, 5.0, 10, and 20 μM).

Sample Preparation for Analysis of Specific Activity. AM demethylation activity was determined by measurement of the formation of DHA, according to the method of Asimus and Ashton (2009), with minor modifications. AM stock solution (50 mM) was prepared in CH_3CN/H_2O [50:50 (v/v)], and a working solution (500 μM) was prepared by dilution of the stock solution in potassium phosphate buffer, pH 7.4. The incubation mixture contained AM as a substrate (1 and 50 μM), recombinant P450 enzymes (CYP1A1, CYP1A2, CYP1B1, CYP2A6, CYP2B6, CYP2C8, CYP2C9, CYP2C19, CYP2D6, CYP2E1, CYP2J2, CYP3A4, CYP3A5, and CYP4A11; 0.5 pmol) or human liver microsomes (50 μg), 0.5 mM NADPH, 5 mM $MgCl_2$, and 50 mM potassium phosphate buffer to a final volume of 90 μl. After preincubation (3 min at 37°C), the reaction was started by addition of NADPH. Reactions were performed for 30 min and terminated by the addition of 100 μl of methanol. Then, 5 μl of internal standard (ART at 100 μM) and 100 μl of H_2O were added. The resulting mixture was vortexed. After centrifugation at 12,000*g* for 10 min, 80 μl of the supernatant was transferred to a new plastic tube and passed through a filter (pore size: 0.2 μm; YMC). Then, 10 μl of the filtered solution was injected into the LC-MS/MS system for analysis. All peaks were integrated automatically by Xcalibur software. Levels of DHA were calculated from the calibration curves by using the ratios of their peak areas to that of ART. Formation of DHA was in the linear range between 10 and 60 min and 30 and 50 μg of microsomal protein.

Sample Preparation for Analysis of Kinetic Parameters of CYP2B6 and CYP3A4. AM stock solution (50 mM) was prepared in CH_3CN/H_2O [50:50 (v/v)], and working solutions (0.25, 0.50, 1.25, 2.5, 5.0, 12.5, and 25 mM) were prepared by dilution of the stock solution. These solutions were diluted with 50 mM potassium phosphate buffer, pH 7.4, and the final calibration curves were obtained with 0.5, 1.0, 2.5, 5.0, 10, 25, 50, and 100 μM. CYP2B6 and CYP3A4 activity was evaluated using the concentration ranges 0.5 to 50 and 2.5 to 100 μM, respectively. Samples were prepared as described above.

Determination of DHA and ART Using Online Column-Switching LC-MS/MS. Levels of DHA were determined by the LC-MS/MS method described by Huang et al. (2009), with minor modifications. A Nanospace SI-2 LC system, comprising an LC pump, autosampler, column oven maintained at 40°C, and on-line degasser (Shiseido, Tokyo, Japan), was used. The on-line column-switching valve system consisted of an automated switching valve (six-port valve) connected to pump A and pump B. Pump A was connected via the switching valve to the trap column, a CAPCELL PAK C18 SG II (10 × 2 mm i.d., 3-μm particle size) (Shiseido, Tokyo, Japan), and pump B was connected via the switching valve to the analytical column, a Sunfire C18 (150 mm × 2.1 mm i.d., 3.5-μm particle size) (Waters, Milford, MA). The outlet of the analytical column was connected to the mass spectrometer via a divert valve.

Sample loading. A 10-μl aliquot of sample was injected onto the trap column using pump B with the switching valve in position 1. Impurities on the trap column were eluted to waste using 0.1% $HCOOH\text{-}H_2O/CH_3CN$ [5:95 (v/v)] at a flow rate of 200 μl/min for 4 min. Concurrently, initial flow was maintained by pump A at 200 μl/min with 10 mM $HCOONH_4\text{-}H_2O$ (adjusted to pH 4.1 using HCOOH)-0.1% $HCOOH\text{-}CH_3CN$ [20:80 (v/v)] via the analytical column.

Sample elution. At 4 min, the switching valve was switched to position 2 to allow the purified DHA and ART to be eluted from the trap column onto the analytical column and subsequently into the mass spectrometer. Isocratic flow was maintained by pump B at a rate of 200 μl/min for 11 min. Concurrently, the flow from pump A was passed through the trap column and diverted directly to waste. At 11 min, the switching valve was switched back to position 1, and the configuration of the online column switching system reverted back to that in the initial conditions (described for the sample loading above). A divert valve was used to divert the LC effluent to waste during the first 4.5 min and last 0.5 min of the chromatographic run. The total run time was 11 min.

Quantification analyses by MS were performed in the selected reaction monitoring mode because of the high selectivity and sensitivity of selected reaction monitoring data acquisition, in which the transitions of the precursor ion into the product ion were monitored: *m/z* 302 → 145 and 302 → 267 for DHA and *m/z* 300 → 151 and 300 → 209 for ART. The optimized parameters for MS are as follows: positive heated electrospray ionization voltage, 3 kV; heated capillary temperature, 300°C; sheath gas pressure, 50 psi; auxiliary gas setting, 20 psi; and heated vaporizer temperature, 300°C. Both the sheath and auxiliary gases were nitrogen. The collision gas was argon at a pressure of 1.5 mTorr. The LC-MS/MS system was controlled by Xcalibur software, and data were also collected with this software. The retention times of DHA and ART were 7.0 and 7.5 min, respectively.

Liver Specimens. Human liver specimens were obtained from the Human and Animal Bridging Research Organization (HAB) in Chiba, Japan, using frozen human livers (most of the donors were white). Microsomes were prepared from these specimens using differential centrifugation. Research protocols were approved by the ethics committees of the Graduate School of Pharmaceutical Sciences, Tohoku University (Sendai, Japan).

Expression of CYP2B6 Variant Proteins in COS-7 Cells. CYP2B6 variant proteins were expressed in COS-7 cells as described by Watanabe et al. (2010).

Determination of Protein Expression Levels by Immunoblotting. Western blotting was performed according to standard procedures, with 10% SDS-polyacrylamide gel electrophoresis, and 30-μg microsomal fractions were loaded into each lane. Recombinant CYP2B6 Supersomes reagent (BD Gentest) was coanalyzed as the standard on each gel and used to quantify the CYP2B6 protein. The CYP2B6 protein was detected using the antihuman CYP2B6 antibody (BD Gentest) and horseradish peroxidase-conjugated goat anti-rabbit IgG (Dako Denmark A/S, Glostrup, Denmark). CYP3A4 Baculosomes reagent (Invitrogen) was coanalyzed as the standard on each gel and used to quantify the CYP3A4 protein. The CYP3A4 protein was detected using the antihuman CYP3A4 antibody (Nosan, Yokohama, Japan) and horseradish peroxidase-conjugated goat anti-rabbit IgG (Dako Denmark A/S). Immuno-

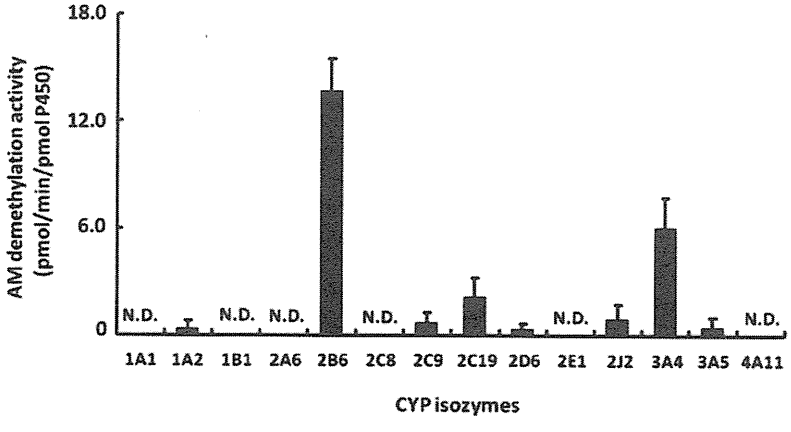

FIG. 3. AM demethylation activity of 14 P450 isozymes. The concentration of AM was 50 μM. Each number corresponds to a P450 subtype. Results are presented as the mean ± S.D. in triplicate. N.D., not detectable (activities were lower than 0.22 pmol · min^{-1} · pmol $P450^{-1}$).

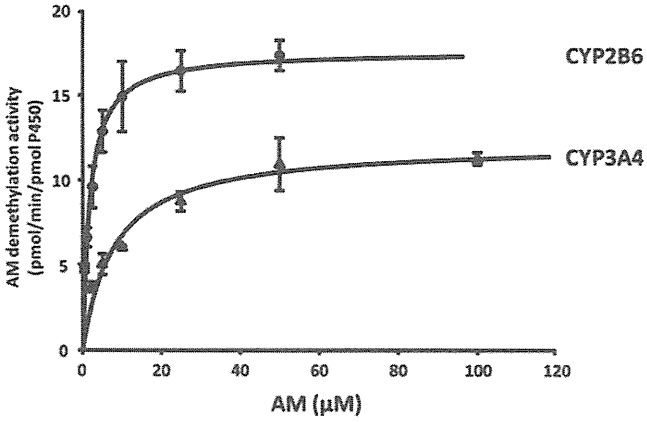

FIG. 4. The Michaelis-Menten curves for the demethylation of AM with recombinant CYP2B6 and CYP3A4.

blots were developed using the SuperSignal West Dura Extended Duration Substrate (Thermo Fisher Scientific). Chemiluminescence was quantified using a lumino-imaging analyzer (LAS-1000; Fujifilm, Tokyo, Japan) and ImageJ software (National Institutes of Health, Bethesda, MD).

Sample Preparation for Analysis of Kinetic Parameters of CYP2B6 Variants. Microsomal fractions (50 μg) obtained from COS-7 cells were used for evaluation of the activity of CYP2B6 variants. Samples were prepared as described above.

Statistical Analysis. Apparent K_m and V_{max} parameters were determined using nonlinear regression analysis. All data are the mean ± S.D. in triplicate. Statistical analyses of enzymatic activities and kinetic parameters were performed by analysis of variance using the Dunnett method. $P \leq 0.05$ was considered significant.

Results

AM Demethylation by Recombinant Human P450s. The activities of AM demethylation were measured in 14 recombinant human P450 enzymes (CYP1A1, CYP1A2, CYP1B1, CYP2A6, CYP2B6, CYP2C8, CYP2C9, CYP2C19, CYP2D6, CYP2E1, CYP2J2, CYP3A4, CYP3A5, and CYP4A11) at 1 and 50 μM substrate concentrations. The lower concentration used was intended to approximate the plasma AM concentrations reported to be clinically relevant (0.3–1 μM) (Ali et al., 2010). At 1 μM AM, AM demethylation activities of recombinant CYP2B6 and CYP3A4 were 6.61 and 2.50 pmol · min^{-1} · pmol P450^{-1}, respectively. Under the lower substrate conditions used in this study, DHA was not formed by the other P450 isoforms with the exception of CYP2B6 and CYP3A4. At a higher concentration (50 μM), AM was principally metabolized by CYP2B6, followed by CYP3A4. A low rate of demethylation was observed for CYP1A2, CYP2C9, CYP2C19, CYP2D6, CYP2J2, and CYP3A5; CYP1A1, CYP1B1, CYP2A6, CYP2C8, CYP2E1, and CYP4A11 were inactive (Fig. 3).

Kinetics of AM Demethylation by CYP2B6 and CYP3A4. The kinetics of AM demethylation were investigated for each of recombinant enzymes CYP2B6 and CYP3A4 by Michaelis-Menten plots (Fig. 4). Apparent K_m, V_{max}, and V_{max}/K_m values for CYP2B6 were estimated to be 1.95 μM, 17.9 pmol · min^{-1} · pmol P450^{-1}, and 9.19 μl · min^{-1} · pmol P450^{-1}, respectively; those for CYP3A4 were 8.24 μM, 12.3 pmol · min^{-1} · pmol P450^{-1}, and 1.49 μl · min^{-1} · pmol P450^{-1}, respectively, demonstrating a higher K_m and lower V_{max}, which resulted in an approximately one-sixth V_{max}/K_m value for CYP3A4 relative to that for CYP2B6.

Comparison of AM Demethylation Activities (at 50 μM AM) to Immunoquantified CYP2B6 and CYP3A4 Protein Levels in 13 Human Liver Microsomes. As shown in Fig. 5, AM demethylation activity in 13 human liver microsomes was correlated with immunoquantified CYP2B6 content ($r^2 = 0.548$, $P = 0.004$) but not with immunoquantified CYP3A4 content ($r^2 = 0.109$, $P = 0.272$).

Enzymatic Properties for AM Demethylation by Wild-Type and 25 Variant CYP2B6s. The demethylation activities of wild-type and 25 variant microsomal CYP2B6 proteins were determined using AM (50 μM) as a substrate (Fig. 6). For CYP2B6.8, CYP2B6.12, CYP2B6.18, CYP2B6.21, and CYP2B6.24, no AM demethylation activity was detected. The enzymatic activity of CYP2B6.3 could not be calculated because its expression level could not be determined by immunoblotting. CYP2B6.10, CYP2B6.11, CYP2B6.14, CYP2B6.15, CYP2B6.16, CYP2B6.20, and CYP2B6.27 exhibited significantly decreased activities compared with that of wild-type CYP2B6.

The Michaelis-Menten kinetics for AM demethylation were determined for CYP2B6.1, CYP2B6.2, CYP2B6.4, CYP2B6.5, CYP2B6.6, CYP2B6.7, CYP2B6.9, CYP2B6.10, CYP2B6.13, CYP2B6.14, CYP2B6.17, CYP2B6.19, CYP2B6.20, CYP2B6.23, CYP2B6.25, CYP2B6.26, and CYP2B6.27. The kinetic parameters are summarized in Table 1. The estimated kinetic parameters, apparent K_m, V_{max}, and V_{max}/apparent K_m for AM demethylation by CYP2B6.1 were 3.10 μM, 36.0 pmol · min^{-1} · pmol CYP2B6^{-1}, and 12.4 μl · min^{-1} · pmol CYP2B6^{-1}, respectively. The V_{max} values for CYP2B6.14, CYP2B6.20, and CYP2B6.27 were significantly decreased, whereas those for CYP2B6.2, CYP2B6.4, and CYP2B6.6 were significantly increased, relative to that for the wild-type enzyme.

Discussion

In this study, we have determined the human P450 enzymes responsible for AM demethylation. Among 14 human P450s, CYP2B6

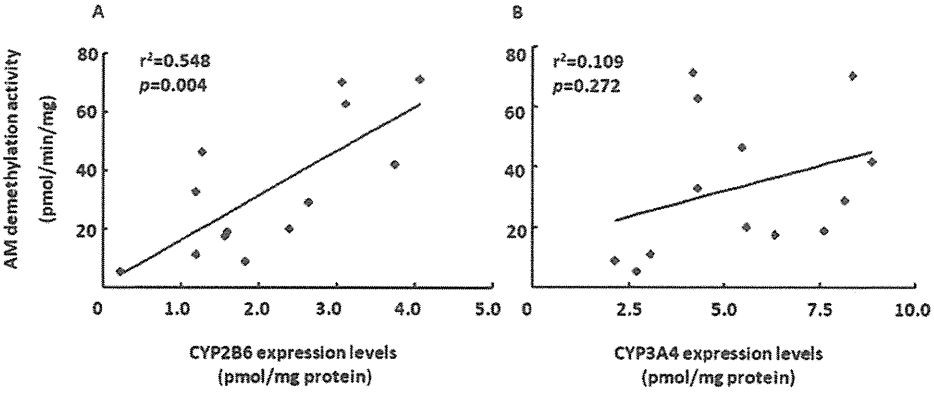

FIG. 5. Comparison of AM demethylation activities (at 50 μM AM) to immunoquantified CYP2B6 (A) and CYP3A4 (B) protein levels in 13 human liver microsomes. Correlation coefficients (r^2) obtained in these cases are shown.